AN INVESTIGATION OF THE APPLICABILITY OF LIMIT DESIGN TO COLD-FORMED, LIGHT GAGE BOX BEAMS

A THESIS

Presented to

The Faculty of the Division of Graduate Studies and Research

by

Jerry Lynn Householder

In Partial Fulfillment

of the Requirements for the Degree

Doctor of Philosophy in the

School of Civil Engineering

Georgia Institute of Technology

June, 1976

D-768-3-2

AN INVESTIGATION OF THE APPLICABILITY OF LIMIT DESIGN TO COLD-FORMED, LIGHT GAGE BOX BEAMS

Approved:

Paul H. Sanders, Director

Barry J. Goodno

William J. Lnenicka

A. Bert Caseman

K.M. Will

Date Approved by Chairman 8/27/76

ACKNOWLEDGMENTS

The writer would like to express his appreciation to his advisors, Dr. P.H. Sanders, Dr. A.B. Caseman, Dr. B.J. Goodno, Dr. W.J. Lnenicka, and Dr. K.M. Will for their guidance and advice. Thanks are due to the Bethlehem Steel Corporation for supplying the materials used and to the Atlantic Steel Company for fabricating the test sections.

TABLE OF CONTENTS

LIST OF FIGURES

LIST OF FIGURES CONTINUED

LIST OF FIGURES CONTINUED

LIST OF TABLES

LIST OF SYMBOLS

A_f - area of compression flange

D - flexural rigidity of a plate

E - modulus of elasticity

E' - strain-hardening modulus

F - Airy's stress function

F_{CF} - force in compression flange

F_y - specified yield stress

G - shear modulus

G' - shear modulus in yielded zone

I - moment of inertia

K - buckling constant

L - length of a member

M_{max} - maximum measured moment

M_P - plastic moment with section fully effective

M_u - theoretical ultimate moment

M_{yield} - moment at yielding of outer fibers

R - rotation capacity

b - flat width of beam

b_e - effective width of compression flange

b_e' - effective width of compression side of web-fully plastic theory

b_e'' - effective width of compression side of web-semi-elastic theory

b_e''' - effective width of top half of web-stiffened theory

LIST OF SYMBOLS (Continued)

c	-	depth to neutral axis from top of beam
d	-	depth of beam
h	-	ratio of strain-hardening stiffness to elastic stiffness
L'	-	width of longitudinal stiffener
p	-	a simplifying variable equal to $b+2d-b_e-6.54$
q	-	lateral load
s	-	ratio of strain at beginning of strain-hardening to strain at yield stress
t	-	plate thickness
w	-	plate deflection
x	-	distance along longitudinal axis of plate
y	-	distance along transverse axis of plate
ε	-	strain
ε_u	-	ultimate compressive strain
ε_y	-	strain at yield stress
μ	-	Poisson's ratio
σ	-	normal stress
σ_{cr}	-	critical buckling stress
σ_{max}	-	the average stress when the edges of plate reach the yield stress
σ_x	-	normal stress in x-direction
σ_y	-	yield stress
Θ	-	rotation
Θ_m	-	maximum rotation
Θ_p	-	rotation at yielding of outer fiber

SUMMARY

In the adaptation of ultimate strength analysis and design methods to box beams made from cold-formed steel, two questions must be answered. First, what conditions are necessary in order to assure that a moment-curvature relationship justifying moment redistribution may be attained? Secondly, if suitable relationships are found for beams whose dimensions dictate effective width analysis, what is the ultimate moment capacity?

Fourteen tests were run on box beams to study their behavior. Nine beams were stiffened by longitudinal stiffeners in the flanges. Five beams had longitudinal stiffeners in their webs.

Of the nine beams with flange stiffeners, the five whose web depth-thickness exceeded $412/\sqrt{F_y}$ (the current AISC specification for plastic design sections) did not develop suitable moment curvature relationships. All five sections with web stiffeners developed suitable relationships regardless of the dimension-thickness ratios. Suitable theories for the prediction of the ultimate moment capacity were developed. Finally, recommendations for design and further research were made.

CHAPTER I

INTRODUCTION

Definition of the Problem

During the past three decades, a great deal of research has been performed demonstrating the applicability of ultimate or plastic analysis and design methods to steel structures. Most of this research has concentrated on conventional wide flange rolled shapes and has resulted in specifications for geometric properties of these shapes which are based on stability criteria. Other significant results of this research are (a) bracing requirements for the compression flanges of beams subject to bending moment and (b) stability parameters for columns subject to axial compression and, possibly, bending moment. The relationships derived from research results first appeared in the "Specifications for the Design, Fabrication and Erection of Structural Steel for Buildings" of the American Institute of Steel Construction in 1963 (35) and have since then been widely adopted by many building codes in the United States.

However, not all steel structural members are fabricated from conventional wide-flange shapes; some members which are subject to relatively low forces and moments

can be economically made from sheet steel which is bent at room temperature (cold-formed) into the shape of a hollow box. Such members have stability characteristics generally superior to wide flange sections of equal weight. It would thus appear that ultimate design methods may be more practicable for such members than for wide flange shapes.

The stability of hollow box sections with regard to local buckling is known to increase as width-thickness and depth-thickness ratios decrease. However, moment of inertia and section moduli (elastic and plastic) decrease as these ratios decrease, and the resulting stresses due to a given loading increase. These phenomena can form the basis for a complex problem in optimization which is stated simply: how large can width-thickness and depth-thickness ratios become before the rate of loss of stability becomes greater than the rate of increase of the plastic section modulus? The research described herein pertains to the answer to this question. Another problem which is considered is that of the effect of longitudinal stiffeners which may be necessary in the fabrication of hollow box sections of the type used in this research.

Historical Aspects of Structural Design

In the earliest days of structural design, "engineers" designed structures on the basis of their experience and intuitive feeling for structural behavior.

Although theoretical analysis is presently a part of all structural design, experience still plays an important part in specification writing. As analytical methods of elastic stress analysis became popular, the engineer's attention was focused more and more on the individual members rather than on the structure as a whole. For steel structures, the primary criterion for design was the limiting of actual stress in the structure so as not to reach the yield point. If the attainment of the yield stress at some isolated point within the structure constitutes failure, then much of the currently accepted design practice which is considered to fall within the realm of elastic design would have to be abandoned. As a consequence of factors such as residual stress, stress concentrations, and redistribution of stress, local plastic flow is inevitable in many structures designed on any basis.

Many engineers have long recognized that the design of structures on the basis of allowable stresses in the individual members does not permit proper consideration of the factor of safety against collapse.

Ultimate design concepts as they are presently understood were first applied to the design of several apartment buildings in 1914. In the design of these buildings the ultimate collapse was determined to occur at some multiple of the service load (35). Timoshenko (28)

refers to the work of N.C. Kist who in 1920 proposed a method of determining safe dimensions of steel structures utilizing ultimate load capacity in the plastic range.

Since these early efforts, significant contributions have been made to the ultimate design theory of structures both in the United States and abroad (35). Plastic design is already a part of the AISC specifications (36) chiefly as a result of the research carried out at Lehigh University under the direction of Lynn Beedle.

Plastic design is a procedure based on the maximum load the structure will carry as determined from an analysis of strength in the plastic range. Secondly it consists of consideration of certain limitations which might prevent the structure from attaining the computed maximum load.

Basic Plastic Theory

A basic assumption used in the analysis of bending of an initially straight beam is that a section perpendicular to the longitudinal axis of the beam remains plane as the beam is bent under the influence of an applied moment. Figure 1 shows the stress strain distributions across such a beam if stress is proportional to strain. The constant of proportionality is called Young's Modulus, E. The relative rotation between two cross-sections is θ_1 as shown.

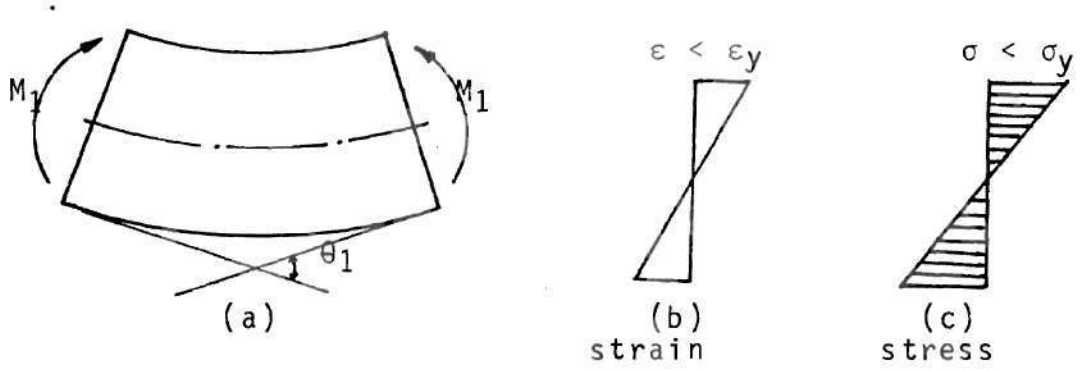

Figure 1. Elastic Stress Distribution Due to Bending.

As the moment increases to M_2 which is greater than the yield point moment, $\sigma_y I/c$, the section becomes partially plastic as shown in Figure 2.

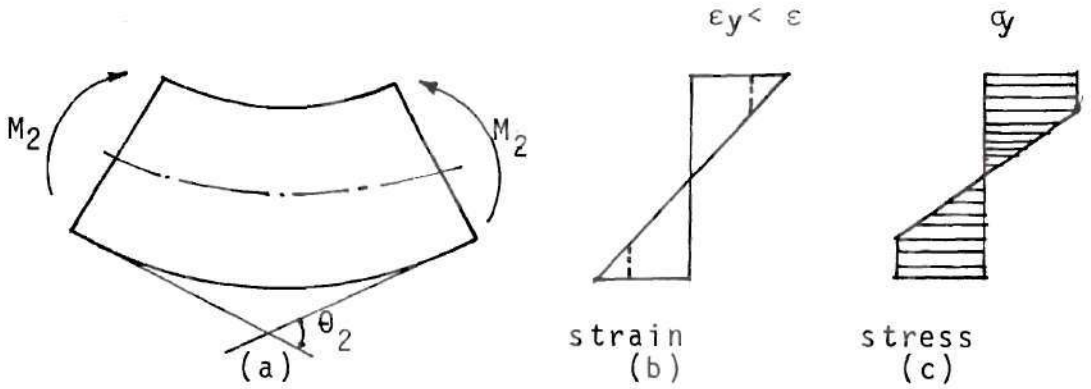

Figure 2. Partially Plastic Stress Distribution Due to Bending.

Assuming an idealized stress-strain relationship (i.e. no strain-hardening) the moment could continue to increase as shown in Figure 3.

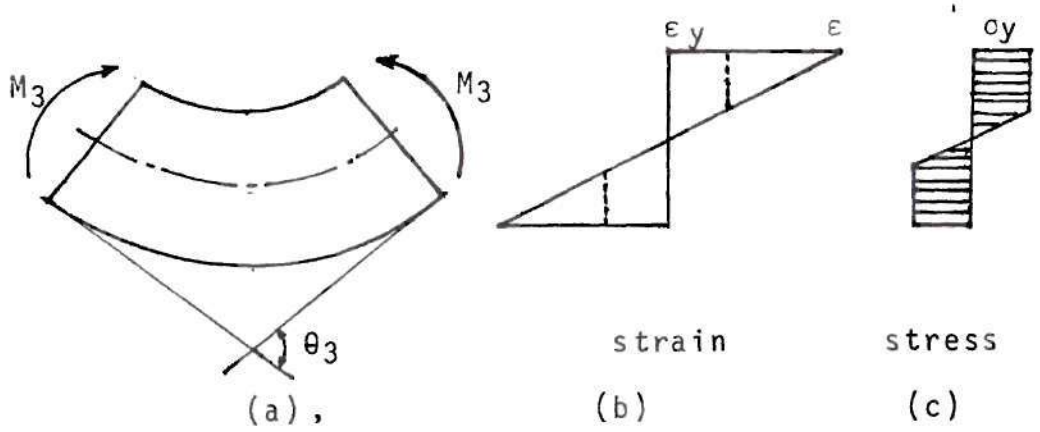

Figure 3. Partially Plastic Stress Distribution as M approaches M_p.

When the entire cross-section is fully plastic as shown in Figure 4, the ultimate moment, M_p, is reached.

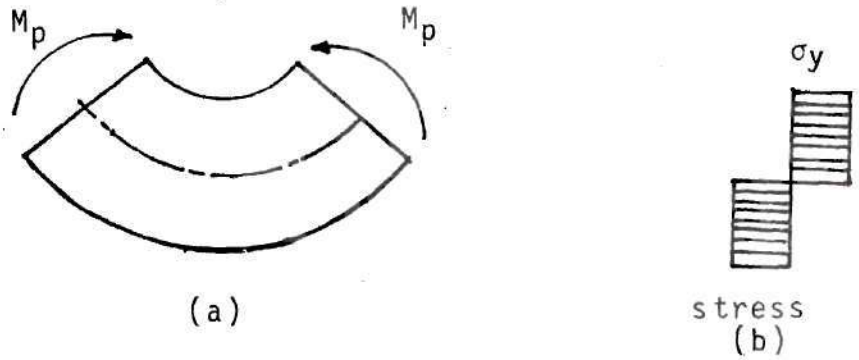

Figure 4. Fully Plastic Stress Distribution.

At this point the region of yielding will have reached the neutral axis, and a plastic hinge is said to exist. Due to the ductility of structural steel, inelastic rotation at the hinge may occur neglecting any stability considerations.

In statically indeterminate structures, when a plastic hinge is formed no more moment can be imposed at that section. Consequently as load is added, moments are redistributed to other parts of the structure where plastic hinges do not yet exist. Finally hinges are formed at other points within the structure forming a collapse mechanism. A design based upon the ultimate collapse load is a design in which the true factor of safety against collapse is known.

Stability Considerations in Plastic Design

A necessary condition which must be satisified in order to justify the use of plastic design procedures is that the ultimate moment, M_p, at each plastic hinge location maintain its full value until sufficient additional sections have yielded, through the redistribution of moments, to produce a mechanism. In other words, in plastic design it is necessary that the moment-rotation curve possess a flat plateau at a level reasonably close to the ultimate moment for some specified distance (Figure 5).

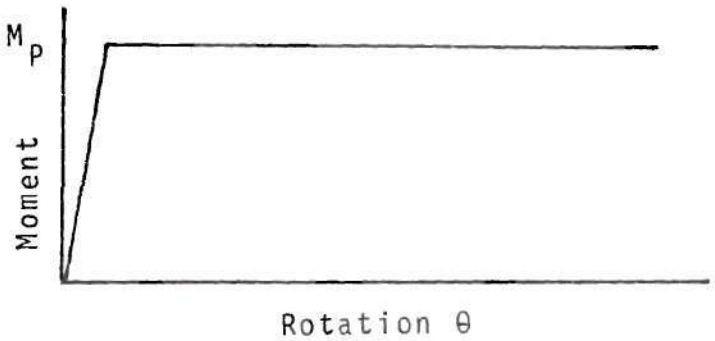

Figure 5. Idealized Moment Curvature Relationship.

Premature reduction in the moment capacity prevents rational analysis. In a properly braced wide-flange beam, this reduction is usually brought on by local buckling of the thin plate elements which comprise the beam. In beams not properly braced against lateral buckling, the beam unloads as soon as lateral-torsional buckling occurs, and no plastic hinge is said to exist beyond this point. Lateral and local buckling are recognized as the basic inherent weaknesses of the wide-flange shape (25).

Tse (30) has demonstrated that a box beam with an unsupported length conceivable in practical applications will not buckle in a lateral-torsional mode under the action of pure bending moments. Also, unlike the wide-flange shape, a box beam does not lose its resistance against lateral-torsional buckling due to penetration of yielding over the cross-section.

The need for adequate bracing against lateral-torsional buckling for beams designed by plastic methods is probably the primary reason that this method is not in wider use today. In areas where the ratio of labor cost to material cost is disproportionately high this consideration can completely obliterate the economics realized by the use of plastic analysis and design.

While local buckling limitations cannot be completely eliminated, they can be liberalized by the use of closed box sections. This is due to the fact that the flange of

a box section is considered to be a stiffened compression element while the flange of a wide-flange beam is unstiffened. The current AISI specifications allow a maximum width-thickness ratio of $190/\sqrt{F_y}$ for the former, and only $65/\sqrt{F_y}$ for the latter. An unstiffened compression element is defined as a flat element which is stiffened at only one edge parallel to the direction of stress. In the case of a wide flange, the web is the stiffener and each side of the flange is an unstiffened compression element. A stiffened compression element is a flat element which is stiffened on both edges parallel to the direction of stress. The stiffeners may be webs, intermediate stiffeners, or simple lips; the compression flange of a box beam is a stiffened compression element.

Further consideration of limiting width-thickness ratios will be presented later.

Rotation Requirements

When the ultimate moment, M_u, of a beam is reached at the first hinge of an indeterminate structure, it is assumed that relative rotation of the segments meeting at the hinge can occur until sufficient additional sections have yielded to form a mechanism. It is necessary that relative rotation, without substantial loss in moment capacity, occurs at all plastic hinge locations in order to obtain a mechanism capable of rational analysis. The rotation,

during which the plastic moment is maintained, is called the rotation capacity (11). The solid curve in Figure 6 shows a typical moment-rotation relationship for a steel beam.

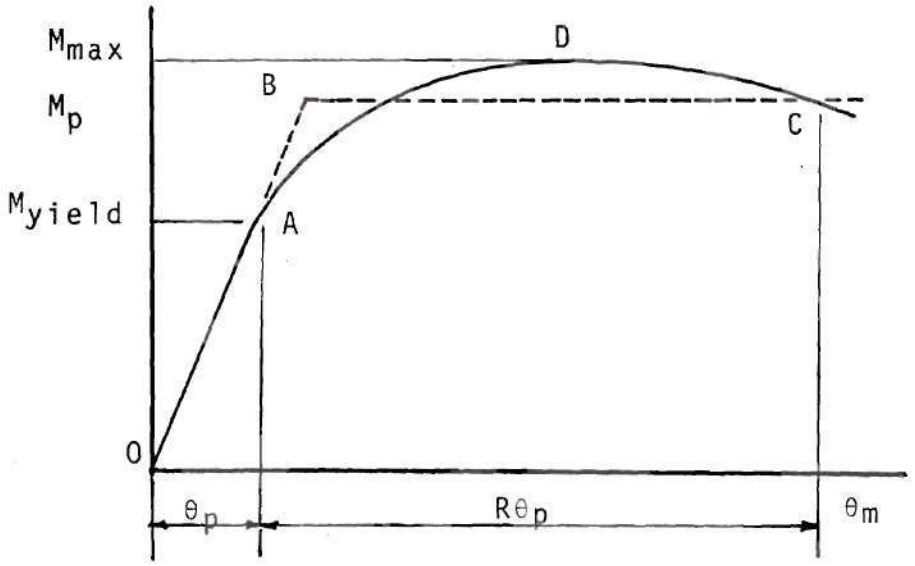

Figure 6. Typical Moment-Rotation Curve

The member first responds along line OA in an elastic manner. From point A to point C the beam behaves in a non-linear manner due chiefly to the following non-linearities:

(1) geometric--changes in force distribution due to deflections.

(2) material--yielding and strain-hardening.

(3) instability--lateral and local buckling.

The actual moment-rotation curve, OADC, is idealized in practice by the straight lines OAB and BC. The rotation capacity is defined as

$$R = \frac{\theta_M}{\theta_P} - 1 \qquad (1)$$

In determining whether the rotation capacity for a particular beam is adequate, it is necessary to know the required hinge rotation for the given structure. Since the required hinge rotation is a function of not only the geometry of the structure but also its loading, there exists an infinite number of cases and hence infinite solutions. For the case of a fixed-end beam of constant cross-section subject to a uniform load, the required hinge rotation capacity is $M_pL/6EI$. This case is solved in the Appendix. Many structures of practical geometric configurations and loadings have been examined, and a general range of required rotation capacities has been found (10, 19).

Furthermore, it has been shown (10) that a load close to the ultimate can be attained with much smaller hinge rotations that those calculated for a complete mechanism. Driscoll (10) has analyzed a two-bay gable frame and found that an angle of 1.52 M_pL/EI was required to form a mechanism. However, 98% of the ultimate load was reached with a rotation of only 0.54 M_pL/EI. As a result of these and similar studies most researchers have accepted

values of rotation capacities ranging from three to four. In comparing the rotation requirements of the two problems just mentioned it is interesting to note that some structures have a zero rotation requirement (i.e. a fixed end beam with concentrated load at midspan).

Current Cold-Formed Steel Practice

Cold-formed steel construction takes its name from the fact that its members are cold-formed in roll brakes or press brakes from flat steel sheets. Cold-formed structural members are generally lighter and have thinner elements than hot-rolled shapes. Residual cooling stressed from hot-rolling or welding significantly influence the behavior of hot-rolled shapes. Such cooling stresses are absent in cold-formed shapes which are instead subjected to selective strain-hardening during their fabrication.

The current practice followed in the design of cold-formed steel structural elements is governed in the United States by the American Iron and Steel Institute and is a result of work instituted at Cornell University in 1939. Based upon this research and practical experience, the first design specification was published by the AISI in 1946 (32).

In the elastic design of hot-rolled shapes, the local buckling phenomenon is considered to constitute failure. The current specification for the design of cold-formed

structural members utilizes the post-buckling strength of thin plate elements in its treatment of stiffened compression elements (39). This treatment consists of using the effective width procedure first suggested by Von Kármán and later refined by Winter (6). This approach considers material to be effectively missing from the cross-section in areas where buckle deformations are large. While effective width relationships for unstiffened compression elements and webs of beams exist (33), they are not presently a part of the AISI code. Instead of being designed by the effective width procedure, unstiffened compression flanges and webs are proportioned by allowable stresses reduced according to their width-thickness ratios. In beams in which the effective width principle is used, all the section properties are calculated as if material were missing from the compression element.

Since the early 1940's cold-formed steel structural members have gained increasing use, especially for low-rise buildings and for areas of larger buildings were the loads were relatively light. Under certain conditions the use of cold-formed steel structural members offers more economy than the heavier hot-rolled shapes. Cold-formed members can be fabricated into a configuration to suit the intended purpose. Also the use of cold-formed sections offers a continuous spectrum of allowable loads, whereas hot-rolled shapes can

offer only discrete values of allowable loads.

Effects of Cold Work in Steel Structural Members

The cold-working of sheet steel when being cold-formed into structural shapes affects its mechanical properties. In general, cold-forming operations produce an increase in the yield point and ultimate strength and a decrease in the ductility. Cold stretching in one direction has a pronounced effect on the mechanical properties of the material, not only in the direction of the stretching but also in the direction normal to it (7). As a result of several projects which investigated the effects of cold-working (7,16,17, 18), the current AISI specification permits the use of an increased allowable stress when a structural member is fabricated by cold-forming (34).

Inelastic Strain Capacity

There has been a considerable amount of research into the effects of local buckling upon the moment curvature relationships of structural members. Local buckling is regarded as isolated plate buckling of the plate elements which make up wide-flange and box shapes. Since wide-flange members traditionally are used for construction of main members of structures, the majority of the research has been in this area. Also since most commercially

available wide-flange shapes have width-thickness ratios which preclude elastic buckling, inelastic local buckling of wide-flange members has received considerable attention. A typical full-range, idealized stress strain curve is shown in Figure 7, in which ε_y = the yield strain, $s\varepsilon_y$ = the strain at commencement of strain hardening, and E/h = the strain-hardening modulus, where h is the ratio of strain-hardening stiffness to elastic stiffness.

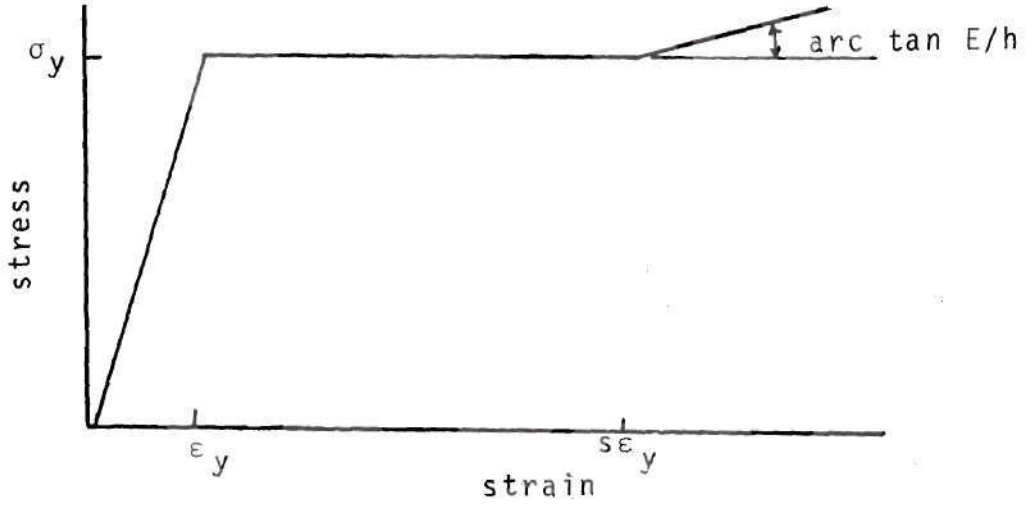

Figure 7. Idealized Stress-strain Relationship.

Stress-strain curves such as that shown in Figure 7 do not adequately represent the true behavior of structural steel. Steel actually yields in a discontinuous manner (24). This phenomenon is a result of the formation of many yield planes such as shown in Figure 8.

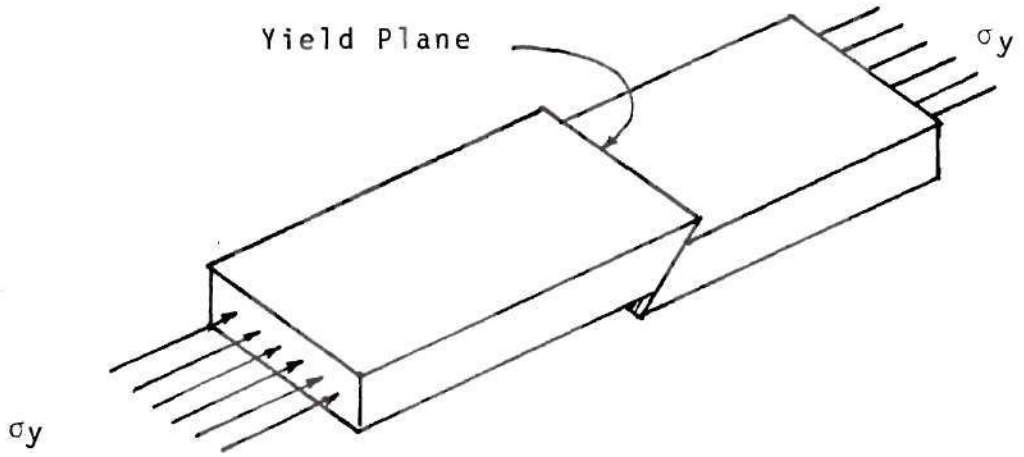

Figure 8. Yielded Flange Element.

These yield planes are regions in which slipping occurs on an atomic level within the metal. The yield planes form along maximum shear planes since the process is simply one of shearing. At the yield plane there is actually a dynamic jump in which the strain at the plane goes from ε_y to $s\varepsilon_y$. Actually no intermediate strains exist between the yield and the strain-hardening strains. The apparent horizontal portion of the stress-strain curve as rendered by the simple tension test represents over-all strains measured over the entire gage length.

Two material properties which must be known in order to solve the flange buckling problem are the yielded "Modulus of elasticity", E', and the yielded shearing

modulus, G'. The value of E' is found directly from the tension test as

$$E' = E/h. \tag{2}$$

The value of G' for the fully yielded condition has been found by Lay (23) to be

$$G' = \frac{2G}{1 + \frac{h}{4(1+\mu)}} \tag{3}$$

Using these properties various researchers have investigated the limiting width-thickness ratios for compression flanges (1,22,23,24). In general these research projects have been aimed at the behavior of unstiffened compression elements. The few studies which have attempted to define the limits of width-thickness ratios for stiffened compression elements have approached the problem empirically (26,21). Reck (26) found that beams with stiffened compression elements whose width-thickness ratios exceeded $221/\sqrt{F_y}$ could not develop ultimate strains substaintially beyond the yield strain. His tests were with steel whose yield stress was 36 ksi. In the use of results such as these, care should be exercised in trying to extrapolate results to all steel strengths. Lay (23) has demonstrated that such extrapolation may be erroneous due to the lower strain-hardening stiffnesses of higher strength steels. Korol (21) whose test specimens consisted of steels with yield strengths of 50 and 55 ksi suggests a limiting value of $150/\sqrt{F_y}$ for the width thickness

ratio. The current AISC specification of compactness of a box shape is $190/\sqrt{F_y}$.

In specifying allowable web depth-thickness ratios, the 1970 edition of the AISC code allowed a maximum ratio of $412/\sqrt{F_y}$ for both compact sections and plastic design sections. Compact sections as defined by Section 1.5.1.4.1 of the AISC specifications are allowed a 10% increase in allowable stress due to their being able to achieve full plasticity. Plastic design sections which are defined in Section 2.7 qualify as such for the same reason. (The maintenance of this moment through some angle of rotation is also requisite as previously discussed.) Supplement No. 3 to the code published in 1974 amended the depth-thickness ratio requirement for compact sections to $640/\sqrt{F_y}$ based on tests on eight plate girders by Croce (9). No adjustment was made, however, to the specification for plastic design sections.

The Ultimate Strength of Compression Elements

The study of the ultimate strength of flat compression elements is essentially a study of large deflection buckling.

The basic equations governing the elastic behavior of flat plates subject to large deflections are as follows:

$$\frac{\partial^4 F}{\partial x^4} + \frac{2\partial^4 F}{\partial x^2 \partial y^2} + \frac{\partial^4 F}{\partial y^4} = E\left[\left(\frac{\partial^2 W}{\partial x \partial y}\right)^2 - \frac{\partial^2 W}{\partial x^2}\,\frac{\partial^2 W}{\partial y^2}\right] \qquad (4)$$

and

$$\frac{\partial^4 w}{\partial x^4} + \frac{2\partial^4 w}{\partial x^2 \partial y^2} + \frac{\partial^4 w}{\partial y^4} = \frac{t}{D}\left[\frac{\partial^2 F \partial^2 w}{\partial y^2 \partial x^2} + \frac{\partial^2 F}{\partial x^2}\frac{\partial^2 w}{\partial y^2} - \frac{2\partial^2 F}{\partial x \partial y}\frac{\partial^2 w}{\partial x \partial y}\right] \quad (5)$$

Together with the appropriate boundary conditions, these equations can be used to find the stress function, F, from which the stresses can be found using

$$\sigma_x = \frac{\partial^2 F}{\partial y^2} \quad (6)$$

and

$$\sigma_y = \frac{\partial^2 F}{\partial x^2} \quad (7)$$

However, due to the fact that the basic equations are fourth order and non-linear, the energy method or an approximate method is commonly used to examine the post buckling behavior of elastic plates.

Since ultimate failure of stiffened compression elements is almost always linked to the occurrence of plastic strains, the problem is further complicated. Graves Smith (13) has examined the ultimate strength of locally buckled columns and demonstrated that failure occurs shortly after the stress at the edge of the plate reaches the yield stress.

In 1932 Von Kármán (31) proposed the effective width approach to the problem of ultimate plate strength. He reasoned that when the ultimate strength is reached, two strips of width $b_e/2$ at each edge carry the yield stress, while the central region remains unstressed.

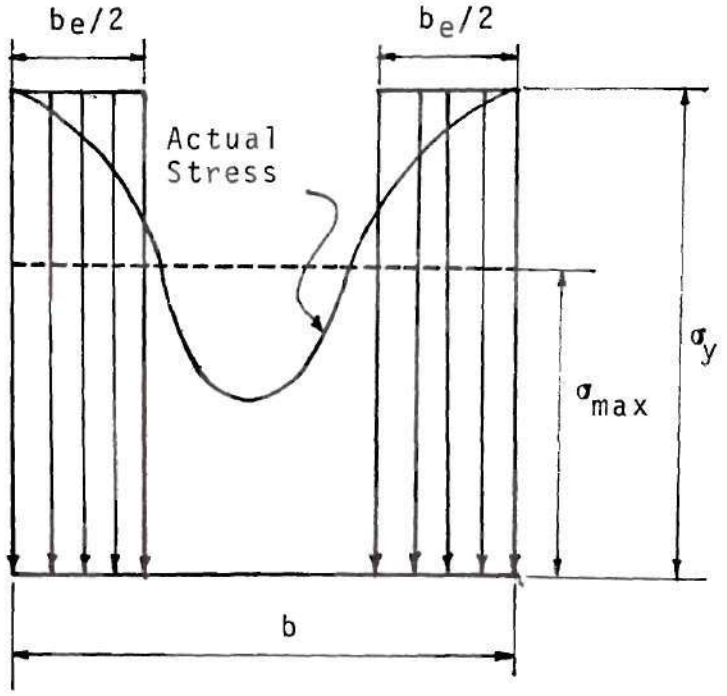

Figure 9. Effective Width of a Buckled Plate.

From this assumption it can be seen that

$$b_e\sigma_y = b\sigma_{max} \tag{8}$$

where σ_{max} is the average stress when the edges reach the yield stress.

The critical buckling stress of the plate is given by

$$\sigma_{cr} = \frac{K\pi^2 E}{12(1-\mu^2)\ (b/t)^2} \tag{9}$$

Von Kármán proposed that failure occurs when the critical stress of the effective plate reaches σy, where

$$\sigma_y = \frac{K\pi^2 E}{12(1-\mu^2)\ (b_e/t)^2} \tag{10}$$

By substitution we have

$$\frac{b_e^2}{b^2} = \frac{\sigma_{cr}}{\sigma_y}, \tag{11}$$

from which the equation

$$\sigma_{max} = (\sigma_{cr} \cdot \sigma_y)^{\frac{1}{2}} \tag{12}$$

can be derived. Since the critical stress, σ_{cr}, can be expressed as a function of $(t/b)^2$, the effective width of a simply supported plate may be expressed as

$$b_e = 1.9\sqrt{E/\sigma_y}\, t \tag{13}$$

Based upon some 150 tests on stiffened compression elements whose width-thickness ratios ranged from 14.3 to 440, Winter (32) proposed the following relationship upon which Formula 16, taken from Section 2.3 of the AISI code is based:

$$b_e = 1.9\sqrt{E/\sigma_y}\left(1-\frac{0.415}{b/t}\sqrt{E/\sigma_y}\right)t. \tag{14}$$

According to the 1968 edition of the AISI code, beams with compression flanges whose width-thickness ratio exceeds

$$b/t = 184/\sqrt{\sigma_y} \tag{15}$$

must be considered to have material missing from the compression flange such that the effective width, b_e, is given by

$$b_e = \frac{253}{\sqrt{\sigma_y}}\left[1 - \frac{50.3}{(b/t)\sqrt{\sigma_y}}\right] t. \tag{16}$$

As a result of this vast amount of work and research, the ultimate strength of the compression flange of a box beam can be very closely determined. However, the determination of the ultimate strength of the webs is very complex. In the case of a box beam with an effective compression flange width, b_e, which is less than the tension flange width, b, the neutral axis will be lowered. Also at loads near the ultimate, the stress distribution in the compression portion of the web is non-linear due to the large deflection of the buckles which occur there. The behavior of the compression portion of the web is not unlike the uniformly loaded plate in which material is considered to be removed. The efforts of many researchers over the years to experimentally check web buckling theories based upon small deflection theory were relatively unsuccessful (15). Basler (2) in studying plate girders with thin webs, suggests an effective section in which a portion of the compression zone of the web is assumed to be nonparticipating. His effective section is shown in Figure 10. Any removal or nonconsideration of material in the web serves to lower the neutral axis further.

In 1964 Walker (32) considered the ultimate strength of rectangular plates subjected to end compression varying from zero at one edge to a maximum at the other as shown in figure 11.

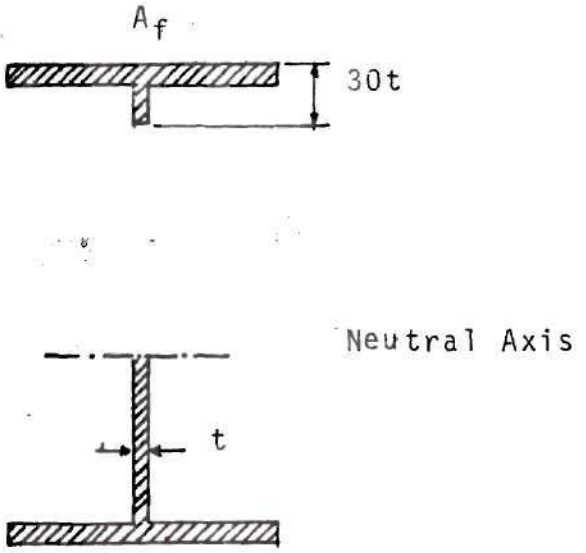

Figure 10. Effective Section of Plate Girder in Bending.

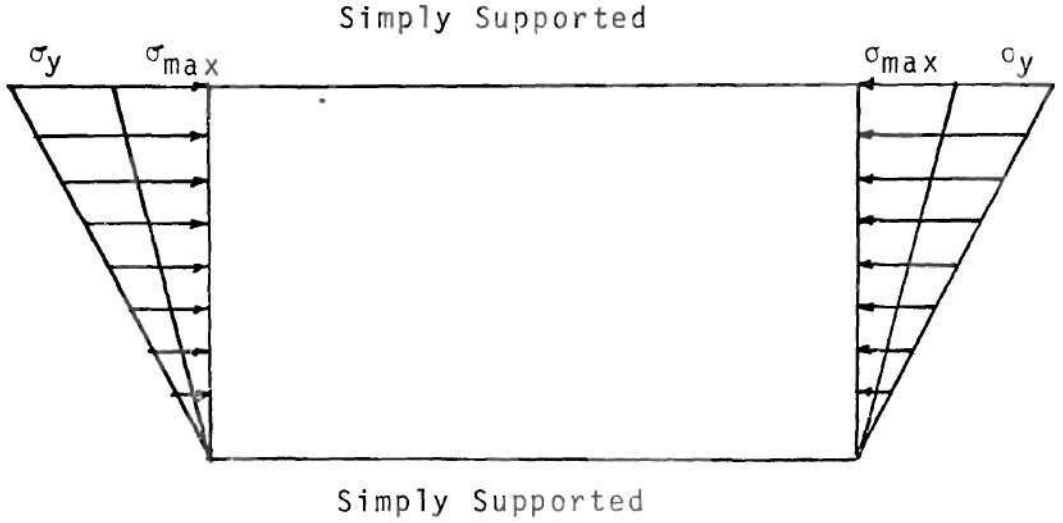

Figure 11. Rectangular Plate Subjected to Varying End Compression.

The results of his work for simply supported plates can be approximated by

$$\sigma_{max} = 0.904 \, (\sigma_{cr}/\sigma_y)^{1/3} \, \sigma_y.$$

The simply supported plate may be thought of as the compression portion of the web.

These and similar ideas will be integrated into theories for the ultimate moment determination of box beams later in this report.

CHAPTER II

INSTRUMENTATION AND EQUIPMENT

Fourteen experiments were performed in this program to study the behavior of box beams made from thin plate elements having longitudinal stiffeners. The structure used in these tests was a simply supported beam which was loaded by two symmetrically spaced vertical loads such that the central portion of the beam was subjected to constant moment. A schematic view of the test structure is shown in Figure 12; the actual structure is shown in Figure 43 in the Appendix.

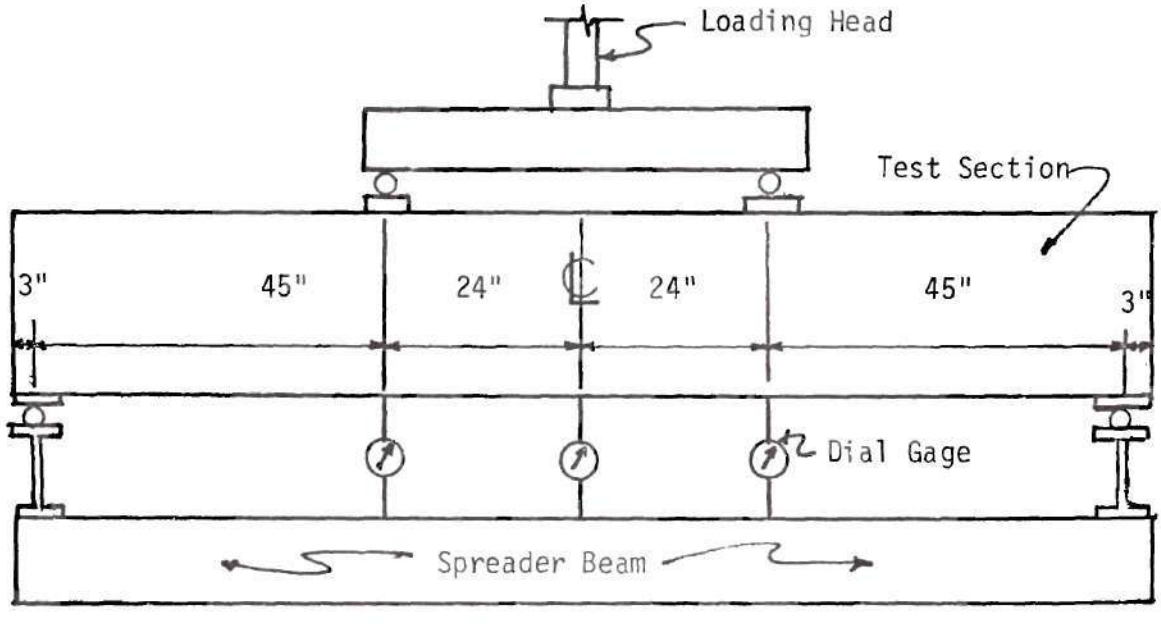

Figure 12. Schematic View of Test Setup.

The test beams were cold-formed in a press-brake. Transverse stiffeners were welded to the beams at points of load application in order to prevent web crippling.

The test machine used in this program was a 450,000 pound screw-fed, universal testing machine manufactured by Riehle.

Deflections in the loading direction were measured during each test by three dial gages positioned as shown in Figure 12. In the elastic range readings were taken at convenient increments of load, while in the inelastic range increments of deformation were used. Loading was stopped each time readings were taken.

In the inelastic range the readings were not taken until sufficient time had elapsed to permit the system to come to rest, and therefore the effects of the rate of loading do not influence the results. The test points in the curves shown in the Appendix represent stable deflection configurations for static loading.

Eleven test sections twelve feet long were fabricated from 14 gage material, while three sections twelve feet long were made from 11 gage material. Each box section was fabricated from two C-sections as shown in Figure 13. Figure 13a shows a beam with the stiffeners located in the webs. Figure 13b shows a beam with the stiffeners located in the flanges. The designation of each beam is

descriptive in that the first two numbers represent the nominal width of the beam in inches, and the second two numbers represent the nominal depth. The letter at the end of the description indicates the location of the longitudinal stiffener--F for flange and W for web. The beams made from 11 gage material are followed by (11). All the test sections studied in this program, along with the pertinent dimensions, are listed in Table 1 of the Appendix.

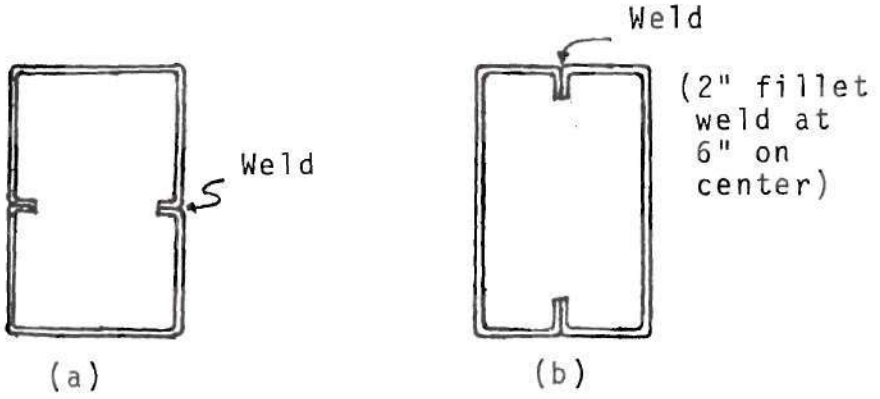

Figure 13. Test Sections.

Since it was the purpose of this program to investigate the moment-curvature relationships of thin box sections, it is important to be able to predict the maximum moment which a beam of this nature can sustain. To aid in formulating a means to predict the beam's ultimate moment carrying

capacity, strain gages were used in two tests--the 1218W and the 1610W. The gages used were SR-4 gages and were attached as shown in Figure 14.

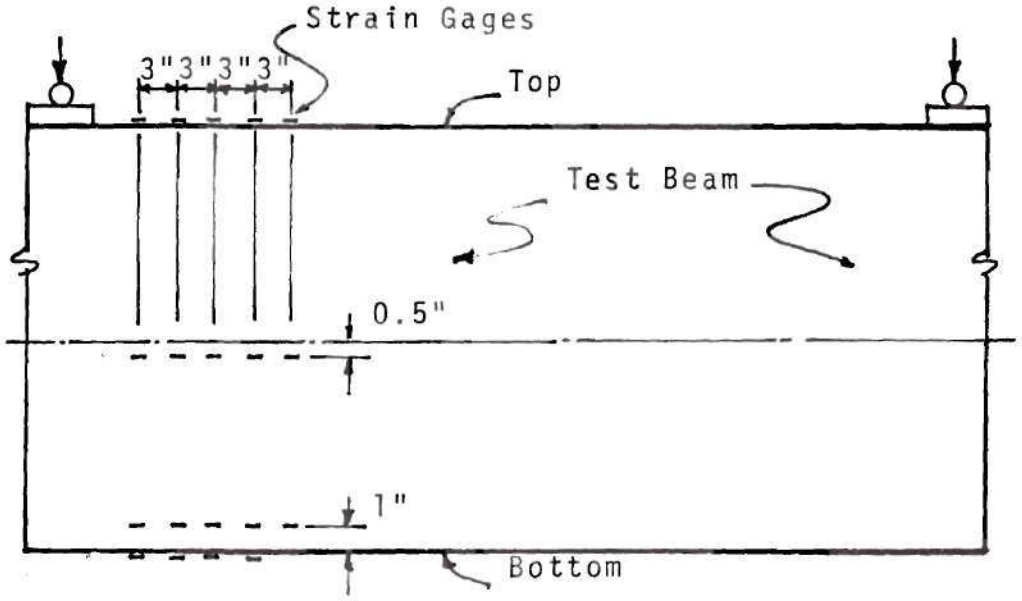

Figure 14. Strain Gage Locations.

Twenty such gages were used in order to have gages at or very near the section where the out of plane buckling was a maximum. The buckling pattern of a stiffened compression element is a series of dish-dome type deformations as shown in Figure 15. At sections a and c the deformations of the compression flange are at a maximum being the dish or inward and dome or outward deformation respectively. At section b there are no out of plane deformations of the plate elements composing the beam. Due to minor variations

which might exist in the location of the neutral axis and stress distribution along the beam, gages were used at several sections in order to determine the strains at a section of maximum buckle deformations,

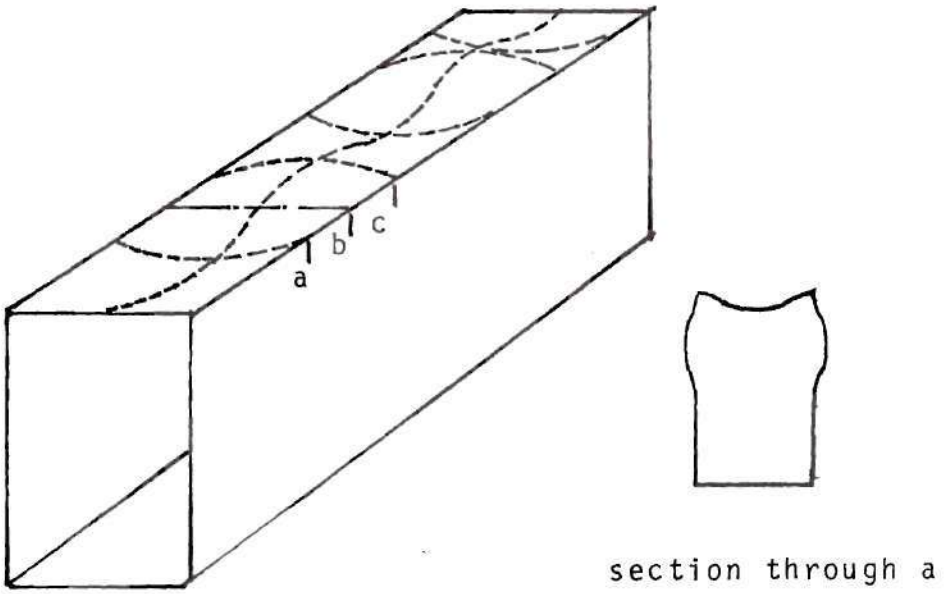

Figure 15. Buckled Configuration of Compression Flange.

The results of the strain gage readings at sections of maximum buckle deflection yield two important results— the stresses at the various locations and the location of the neutral axis. The results of the strain readings are shown for various loadings in Figures 42 and 41 of the Appendix.

Five tensile specimens of standard ASTM shape were tested in self-aligning grips, and strains on a 2 inch gage length were measured by means of an autographic microformer gage. Results of the tests are shown in Figure 39 in the Appendix.

CHAPTER III

RESULTS AND DISCUSSION

Moment-Deflection Curves

In order to qualify as a beam for which ultimate design procedures may be used, the beam must be able to rotate through some given angle with relatively little loss in strength until such time as a mechanism is formed in the structure containing the beam. Moment-curvature tests on wide-flange members which qualify as "plastic design shapes" show a variance from the theoretical plastic moment of as much as 10% (25). For the purpose of the evaluation of the tests in this program, any beam whose capacity falls below 90% of the theoretical ultimate moment before reaching the specified rotation will be considered not to have formed a plastic hinge. A rotation of three times the rotation at the intersection of the elastic and plastic curves will be used as the miminum required rotation (9). The determination of the theoretical ultimate moment capacity will be explained in detail later in this chapter. A curve showing the experimentally observed moment versus the maximum deflection has been drawn for each test section. These curves are shown in the Appendix Figures 25 and 38. Four of the nine sections

in which the longitudinal stiffeners were incorporated into the flanges showed a suitable yield plateau. Of the five flange stiffened sections in which no plastic or ultimate hinge was deemed to have been formed, four sections were non-compact while one section, the Q40BF qualifies as a compact section under the provisions of the AISC (36). Of the five sections in which the longitudinal stiffeners were incorporated into the webs, all were able to develop a usable yield plateau even though none qualified as compact sections under the provisions of the AISC.

In the evaluations of the ultimate moment capacity of thin box sections, three different theories were used, two for the flange stiffened beams referred to as the fully plastic theory and the semi-elastic theory and one for the web-stiffened beams called simply the ultimate strength theory for the web-stiffened beams.

Fully Plastic Theory

The ultimate moment of a box shape in which the depth-thickness ratio of the webs is less than that given by the formula (38)

$$d/t = 412/\sqrt{\sigma_y} \tag{18}$$

and the width-thickness ratio of the compression flange is less than

$$b/t = 190/\sqrt{\sigma_y} \tag{19}$$

can be easily calculated by the principles of plasticity.* Formulas 18 and 19 describe the upper dimension-thickness ratios of shapes defined as "plastic design shapes." Under the provisions of Section 2.7 of the 1969 edition of the AISC code these ratios represent the upper limit beyond which presently accepted plastic or ultimate design procedures may not be used.

In order to predict the ultimate moment capacity of box beams whose width-thickness and depth-thickness ratios exceed the provisions of AISC-2.7, a procedure somewhat similar to that described in Section 2.3 of the AISI code will be used.

The first of the three ultimate strength theories previously mentioned is called the fully plastic theory. In this theory the compression flange is assumed to develop a force of

$$F_{CF} = b_e t \sigma_y = \frac{253}{\sigma_y} \left[1 - \frac{50.3}{\left(\frac{b}{t}\right)\sqrt{\sigma_y}} \right] t^2 \sigma_y \qquad (20)$$

*See Appendix for illustrative example.

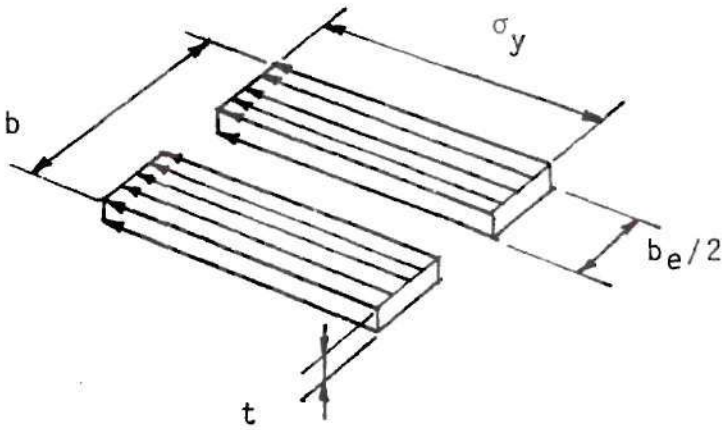

Figure 16. Effective Stresses in Compression Flange.

Figure 16 shows the effective stresses for a beam with no stiffeners. This effective removal of material from the flange lowers the neutral axis to some distance from the top, c. If the compression portion of the web does not buckle (i.e. is fully effective), the final stress state is as shown in Figure 17. This analysis assumes that no unloading of the effective compression flange occurs.

If the web does buckle, its compression side may be considered as a uniformly loaded plate with an effective width of b_e' in the fully plastic state.

$$b_e' = \frac{253}{\sqrt{\sigma_y}} \left[1 - \frac{50.3}{(c/t)\sqrt{\sigma_y}} \right] t \qquad (21)$$

this state of stress is shown in Figure 18.

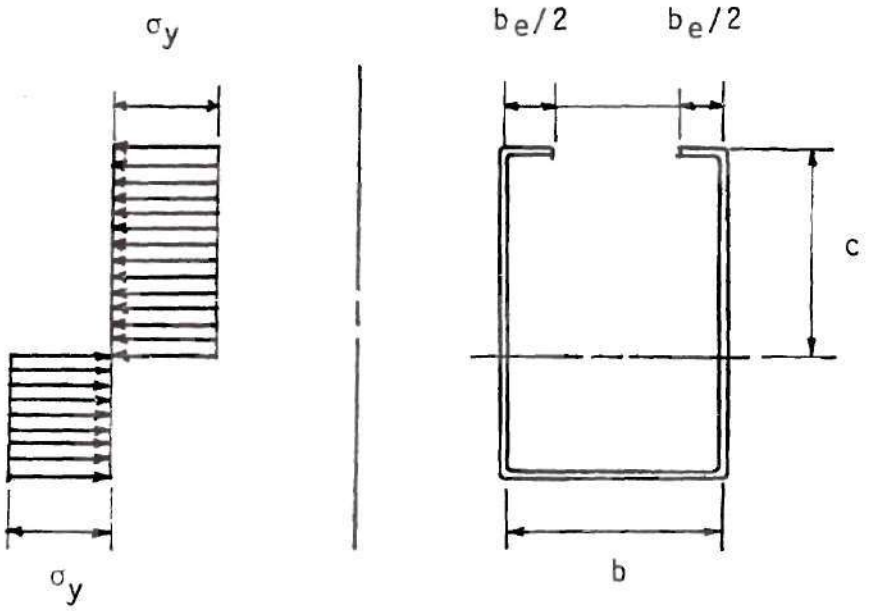

Figure 17. Final Stress State with Web Fully Effective.

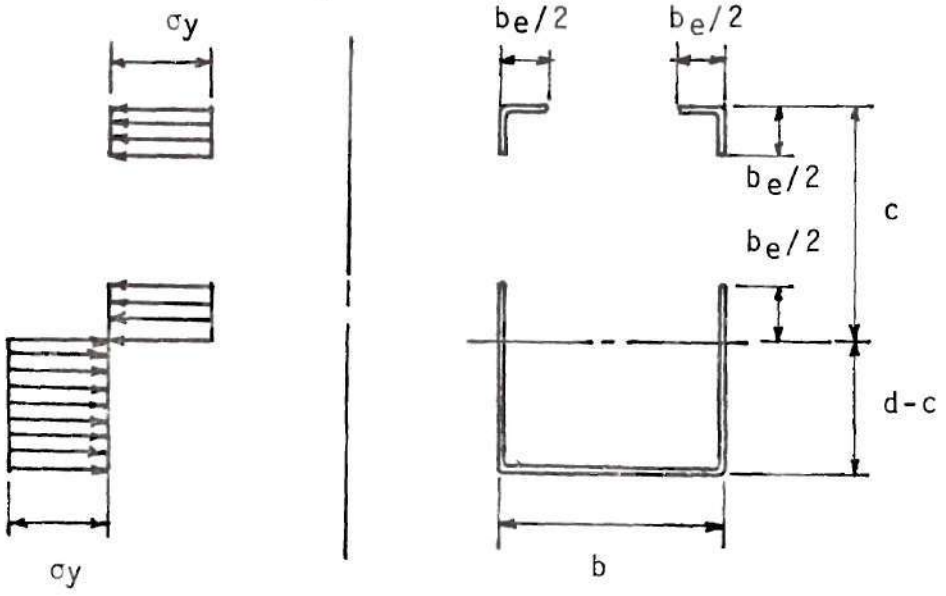

Figure 18. Final Stress State with Web Partially Effective.

The location of the neutral axis for the fully yielded state is found by equating the area above the axis to the area below.

$$b_e = 2b_e' = b + 2(d-c) \tag{22}$$

Combining Formula 16 and Formula 21 with Formula 22 and substituting t=0.0747 in. and σ_y = 33.4 ksi, the depth to the neutral axis, c, is given by

$$c = \frac{p + \sqrt{p^2 + 34}}{4} \tag{23}$$

where

$$p = b + 2d - b_e - 6.54 \tag{24}$$

and the ultimate moment is given by

$$M_u = \left[(b_e + b_e')c + (d-c)^2 + b(d-c) + 2L(d-L')\right] 2.5 \tag{25}$$

for a box beam with longitudinal stiffeners of depth L' in the flanges such as shown in Figure 13b.

The use of this theory is necessarily limited to geometries wherein the results have viable physical significance. For example, consider a beam of constant depth and variable width. As the width increases, the effective width of the compression flange approaches a constant value. The use of Formula 23 could result in a value for the distance to the neutral axis which is greater than the total depth of the beam. This is, of course, a physical impossibility.

In reality the neutral axis must remain above the lower flange. Since the tension force must equal the compression force the tension flange cannot yield for geometries where the tension flange area exceeds the effective compression area. In such cases the following theory governs.

Semi-Elastic Theory

The semi-elastic theory assumes that the compression flange can develop a force, F_{CF}, as given by Equation 20. Substituting E = 29,000 ksi and μ = 0.3 into Equation 9, the critical buckling stress for a simply supported steel plate may be represented as

$$\sigma_{cr} = \frac{104,842}{(b/t)^2} \tag{26}$$

For these same conditions, equation 17 may be rewritten as

$$\sigma_{max} = \frac{42.6\ \sigma_y^{2/3}}{(b/t)^{2/3}} \tag{27}$$

From this equation the effective total force in the compression portion of a single web may be written as

$$F_{EW} = \frac{\sigma_{max}\ c\ t}{2} \tag{28}$$

The assumptions regarding the effective portions of the compression portion of the web are illustrated in Figure 19. The depth from the compression flange to the neutral axis is unknown due to the fact that material may be considered to be removed from the compression flange as well as from the webs. It is assumed that the web is fully effective from the neutral axis to the point at which the stress

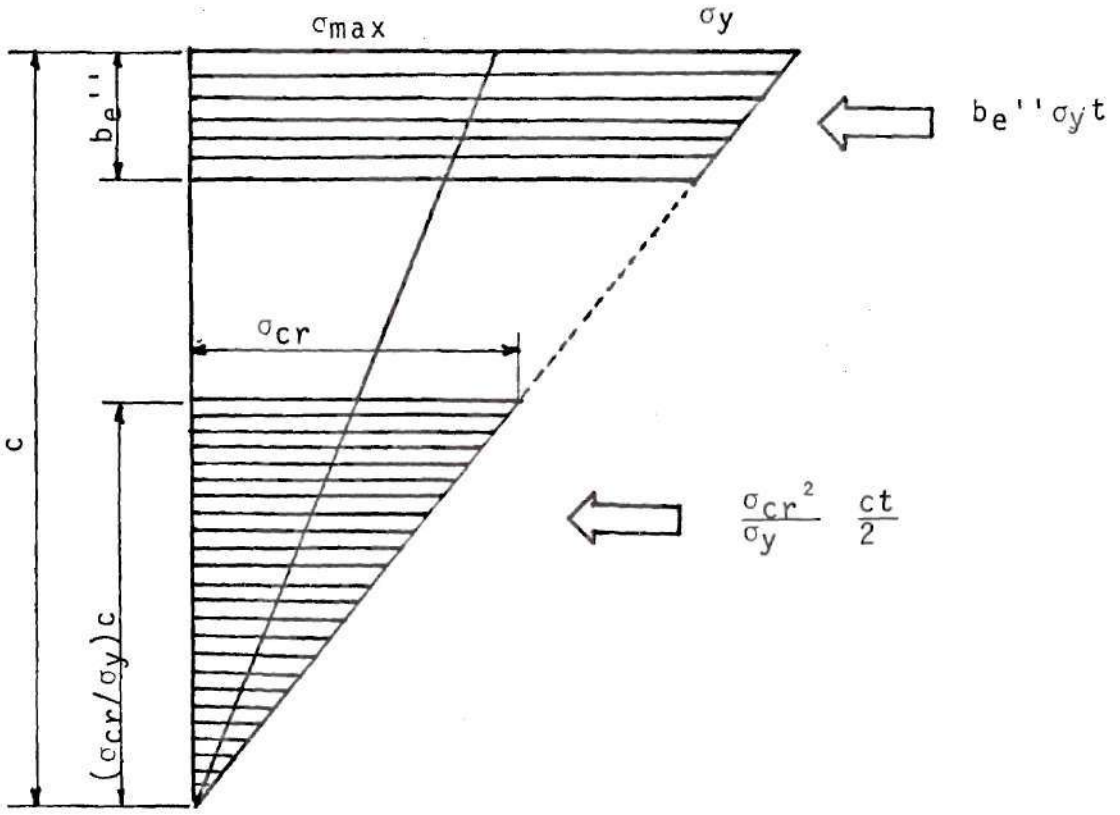

Figure 19. Effective Portions of Compression Side of Web.

reaches the critical buckling stress. Material is considered to be removed from this point to some point a distance of $b_e"$ from the compression flange. This effective width, $b_e"$, is found by equating the effective force in the compression portion of the web found from Walker's work (32), $\sigma_{max} c\ t/2$, with the two forces produced in the assumed effective plate,

$$\frac{\sigma_{max}\ c\ t}{2} = b_e"\ \sigma_y t = \frac{\sigma_{cr}^2}{\sigma_y} \cdot \frac{ct.}{2} \tag{29}$$

Solving,

$$b_e" = \frac{21.3c}{(c/t)^{2/3}\ y^{1/3}} \left(\frac{\sigma_{cr}}{\sigma_y}\right)^2 \frac{c}{2} \tag{30}$$

the webs are found to be fully effective in the use of this theory if

$$\frac{d^2+(b+2L')d}{(2d+b+4L'+b_e)t} < \frac{340.}{\sqrt{\sigma_y}} \tag{31}$$

Figure 20, which shows the assumed effective area at the ultimate load, shows intermediate longitudinal stiffeners in the flanges. If no such stiffeners are present, substitution of L'=0 will yield correct results.

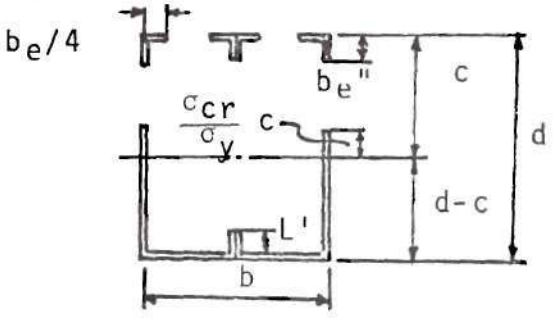

Figure 20. Effective Area Using Semi-Elastic Theory.

The depth to the neutral axis, c, can be found by solving for c in

$$cb_e+2b_e''(c-\frac{b_e'}{2})+(\frac{104842}{\sigma_y(\frac{c}{t})^4})^2c^2+2L(c-\frac{L'}{2})=b(d-c)+(d-c)^2+2L'(d-c-\frac{L'}{2}) \quad (32)$$

Substituting for b_e'' from Equation 30, σ_y=33.4 ksi, and t=0.0747 in, Equation 32 becomes

$$c^2-2.34c^{4/3}-(b+2d+4L'+b_e)c+1.37c^{2/3}-2.0c^{-2}-356c^{-8/3}$$
$$+23100c^{-6} = -(bd+d^2+2L'd) \quad (33)$$

The ultimate moment capacity using this theory is considered to have been achieved when the compression flange reaches its ultimate capacity and the compression portion of the web reaches its ultimate capacity. The theoretical ultimate moment capacity can be calculated by the use of the elastic bending stress formula using the moment of inertia of the effective section and the distance c calculated from Equation 32. The validity of this theory is demonstrated by the tests run. This theory is valid only for beams in which the tension flange does not yield. Therefore it can be seen that the two theories thus far presented are complementary.

Figure 40 in the Appendix shows a plot of the theoretical ultimate moment as derived from the semi-elastic theory divided by the plastic-moment, M_p, as calculated from simple plastic theory, versus depth-thickness ratio for a constant width-thickness ratio. Also superimposed on the same graph is a plot of the theoretical ultimate moment as derived from

the fully plastic theory divided by M_p. Note that for smaller d/t ratios the fully plastic moment gives larger values and is therefore assumed to be correct as previously discussed. For larger d/t values the semi-elastic theory is assumed to be correct.

Loss of Strength in Beams with Unstiffened Webs

It was observed that flange-stiffened beams with large width thickness ratios or large depth-thickness ratios did not maintain a usable moment plateau after the attainment of the ultimate moment. However, for those beams which had longitudinal stiffeners in the webs, a definite and usable moment plateau was observed.

Consider a box beam without web stiffeners, whose depth-thickness and width-thickness ratios dictate the use of effective width analysis in determining the ultimate moment. If the flange buckles first the neutral axis is lowered as shown in Figure 21.

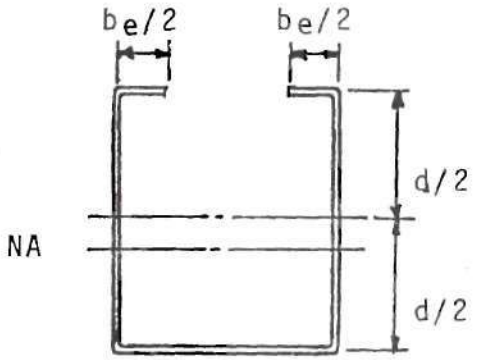

Figure 21. Effective Section with Compression Flange Buckled.

The effect of this lowering of the neutral axis is to increase the depth of the compression side of the web. When the web buckles, material is effectively removed from the compression side of the web as shown in Figure 22.

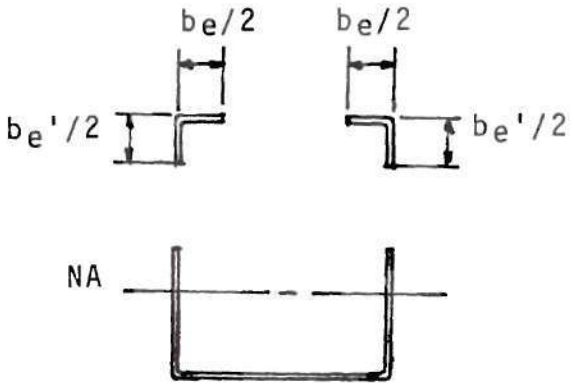

Figure 22. Effective Section with Compression Flange and Web Buckled.

This action lowers the neutral axis even farther. Since the width of the compression side of the web is consequently increased, more material is effectively removed. The net result is that so much material is effectively removed that the beam carries less moment with the edges of the compression flange at yield than when the entire section is effective and the stresses in the beam are less than the critical buckling stress.

As an example, a box beam without longitudinal stiffeners with a width of 4.2 inches and a depth of 10.27

inches, and a thickness of 0.0727 inches is analyzed.* The maximum moment just prior to plate buckling is 193.8 k-in. The ultimate moment from the effective width theory is found to be 154.4 k-in. If the same beam is stiffened by longitudinal stiffeners at the mid-depth of the web, the removal of ineffective material is stopped at some point just above the stiffeners. An analysis of the same beam using stiffeners with zero area, so that the stiffeners will not contribute to the resisting moment, yields a ultimate moment of 199.5 k-in.

Ultimate Strength Theory for Web-Stiffened Beams

In analyzing the ultimate moment capacity of box beams with longitudinal web stiffeners, an effective section as shown in Figure 23 is assumed.

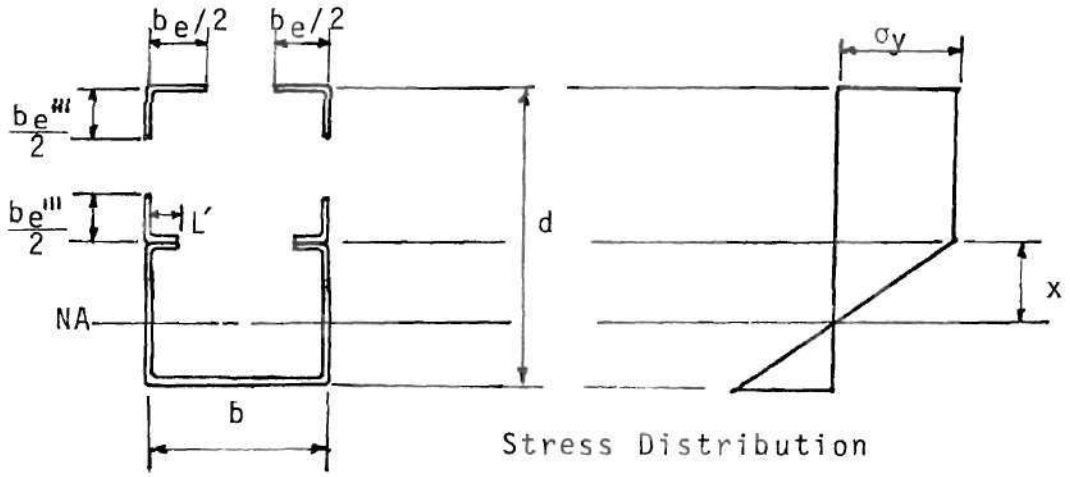

Figure 23. Effective Section of Beam with Web Stiffener.

*The web and the flange buckle simultaneously.

The depth to the neutral axis, x, is found from

$$x = \frac{d(2b+d)}{4(b_e+2b_e'''+4L'+b+d)} \qquad (34)$$

and the resulting ultimate moment is given by

$$M_u = \left[b_e\left(\frac{d}{2}+x\right)+b_e''\left(\frac{d}{2}+2x\right)+4L'x+\frac{2}{3}x^2+\frac{b}{x}\left(\frac{d}{2}-x\right)^2+\frac{2}{3x}\left(\frac{d}{2}-x\right)^3\right]\sigma_y t. \qquad (35)$$

Since the width-thickness ratios exceed $221/\sqrt{\sigma_y}$ the inelastic strain capacity causes the corners to unload (26). This is verified by the strain gage measurements as shown in Figures 41 and 42. In actuality the stress is reduced. However, for analysis purposes it is easier to consider the effective width further reduced. Figure 24 shows this effect. The derivation of this curve is from the experimental results given in the Appendix. The theory used to calculate the theoretical moment for each test is listed in Table 2 in the Appendix.

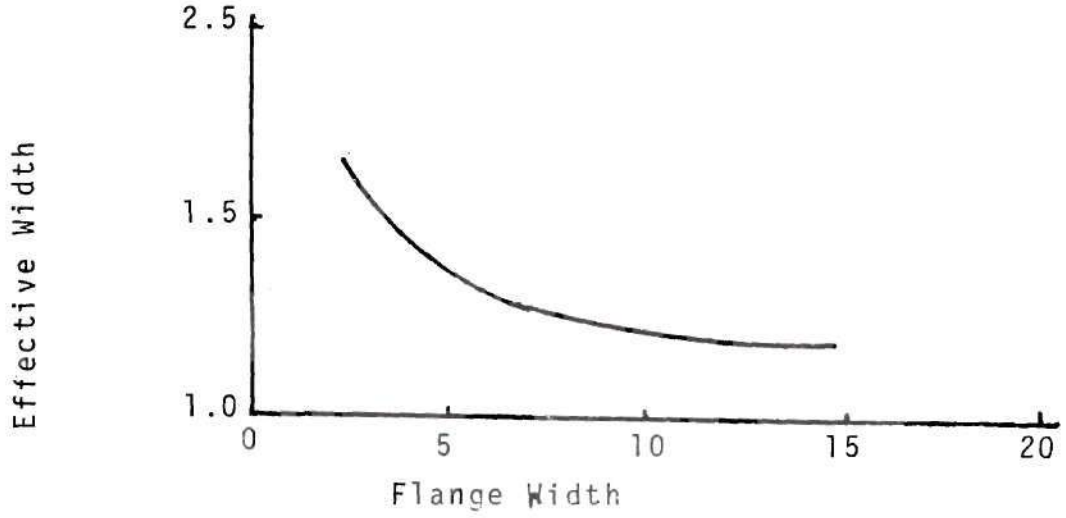

Figure 24. Effective Width for 14 Gage Steel at Ultimate Strains.

CHAPTER IV

CONCLUSIONS

The M-θ curves for four of the nine tests performed on box beams with longitudinal stiffeners in their flanges (Figures 25-33) show an acceptable moment plateau. One of the beams which did not exhibit an acceptable moment plateau meets the requirements of a compact section according to AISC 1.5.1.4.1. The M-θ curves for all five tests performed on box beams with longitudinal stiffeners in their webs (Figures 34-38) show an acceptable moment plateau even though none were classified as compact sections. The ultimate strength of a box beam with thin compression elements may be calculated even though plate buckling occurs prior to the attainment of the ultimate moment.

The use of cold-formed box shapes as members in plastically designed structures is feasible. If no longitudinal web stiffener is used, the sections should conform to the following criteria:

$$\frac{b}{t} < 221/\sqrt{\sigma_y} \qquad (36)$$

and

$$\frac{d}{t} < 412/\sqrt{\sigma_y}. \qquad (37)$$

No apparent material economy is achieved by making the width and depth-thickness ratios of box beams with web stiffeners, greater than that required by Equations 36 and 37.

Box beams can be used as main members to provide a stable and functional structural system in addition to being aesthetically pleasing when left exposed.

Two theories for the calculation of the ultimate moment capacity for beams with flange stiffeners were derived. These theories gave reasonable results in areas wherein each was applicable. The fully plastic theory should be used for the more nearly compact shapes and the semi-elastic theory for beams less compact. The larger value for resisting moment as calculated from either formula will be the proper choice.

Some test sections experienced premature failure due to the crippling of the webs where adequate stiffeners were not provided. In the reproduction of these or similar tests, care should be exercised to insure adequate stiffeners and welds especially in web stiffened members.

CHAPTER V

RECOMMENDATIONS

Further research concerned with limiting depth-thickness ratios needs to be carried out. It is also recommended that the AISC code define the depth of the beam as twice the distance from the neutral axis to the compression side for d/t calculations. There is also a need for further investigation into the minimum moment of inertia of longitudinal stiffeners; premature failure was observed in the testing of the sections of this program due to the early buckling of stiffeners which meet the current AISI standard.

Before any of the findings of this program are incorporated into any standard code, research in the following areas should be carried out:

1. Behavior of box beams subjected to combined shear and bending.
2. Behavior of box beams subjected to combined axial load and bending.
3. Box beams of higher strength steels.
4. Behavior of box beams with the effects of other stiffener types.
5. Behavior of statically indeterminate structures using box beams.

APPENDIX

Table 1. Test Section Dimensions

Section	Width (in.)	Depth (in.)	Stiffener length (in.)	Thickness (in.)
0406F	4.1	5.9	0.8	0.0747
0406F(11)	3.9	5.8	0.8	0.1196
0408F	4.1	7.9	0.8	0.0747
0408F(11)	3.9	7.8	0.8	0.1196
0609F(11)	5.8	8.9	0.8	0.1196
0612F	6.1	12.0	0.8	0.0747
0616F	6.0	16.0	0.8	0.0747
1008F	10.2	8.0	0.9	0.0747
1012F	10.3	12.0	0.8	0.0747
0610W	6.0	9.9	0.8	0.0747
0815W	8.0	15.1	0.8	0.0747
1214W	11.9	14.0	0.8	0.0747
1218W	12.0	18.0	0.8	0.0747
1610W	16.0	10.2	0.8	0.0747

Table 2. Summary of Experimental and Theoretical Moments

Section	M_u (K-in)	M_T (K-in)	d/t	b/t	Theory	Acceptable Yield Plateau
0406F	124.8	121	73.6	21.4	FP	yes
0406F(11)	192.8	208	45.2	13.4	FP	yes
0408F	178.2	170	101.7	21.4	FP	no
0408F(11)	287.8	308	61.9	13.4	FP	yes
0609F(11)	409.7	411	71.1	20.1	FP	yes
0612F	290.0	320	155.3	20.1	FP	no
0616F	389.2	381	208.8	20.1	SE	no
1008F	205.7	192	101.7	61.6	FP	no
1012F	311.6	293	155.3	61.6	FP	no
0610W	171.8	149	125.8	75.0	WS	yes
0815W	265.8	262	195.4	101.7	WS	yes
1214W	256.0	288	182.1	155.3	WS	yes
1218W	343.2	363	235.6	155.3	WS	yes
1610W	181.7	201	125.8	208.8	WS	yes

$190/\sqrt{F_y} = 32.9$; $412/\sqrt{F_y} = 71.3$; $640/\sqrt{F_y} = 110.7$

M_u = Theoretical Moment; M_T = Moment From Tests

FP = Fully Plastic Theory; SE = Semi Elastic Theory

WS = Web-Stiffened Theory

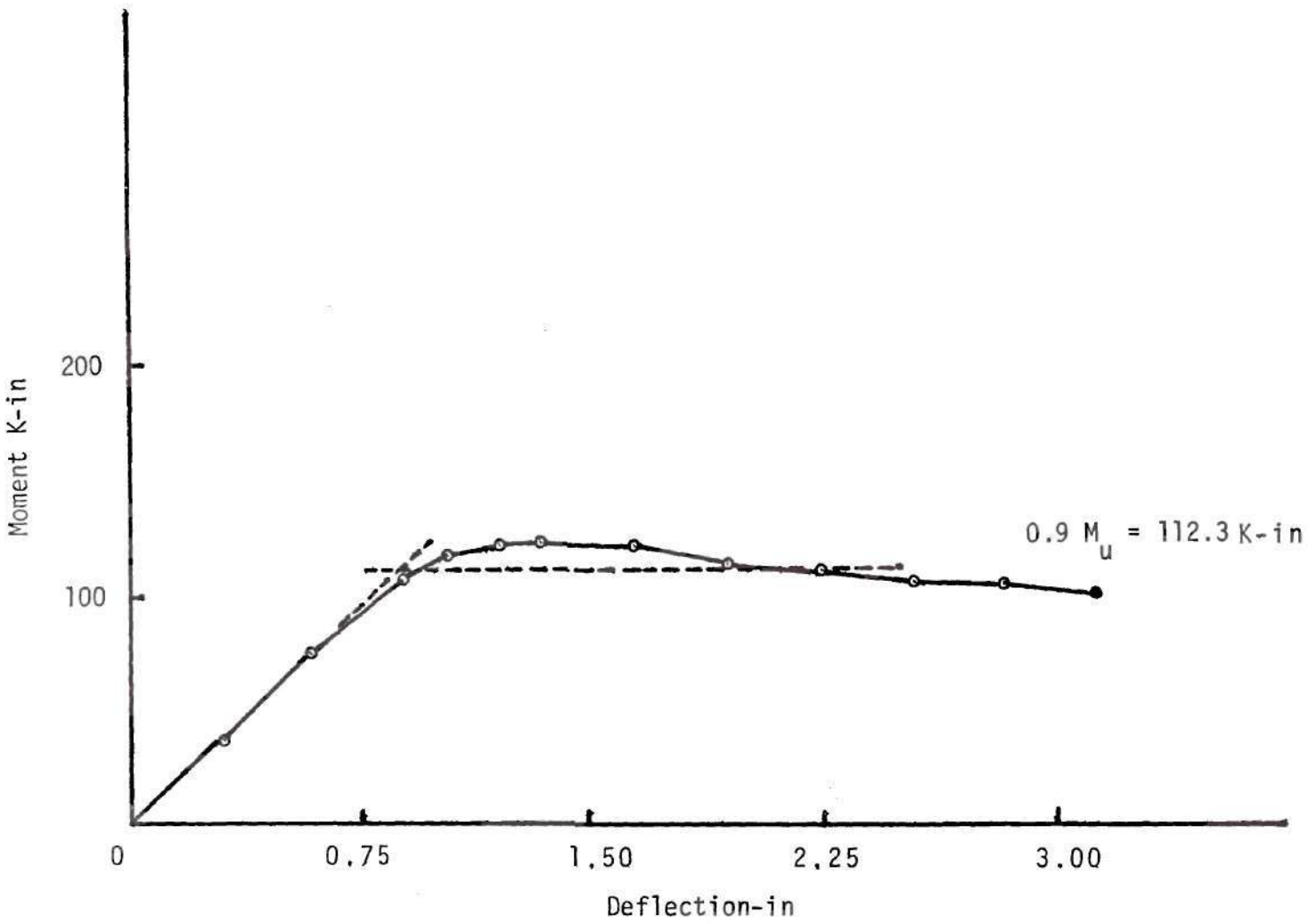

Figure 25. Moment Deflection Relationship--0406F.

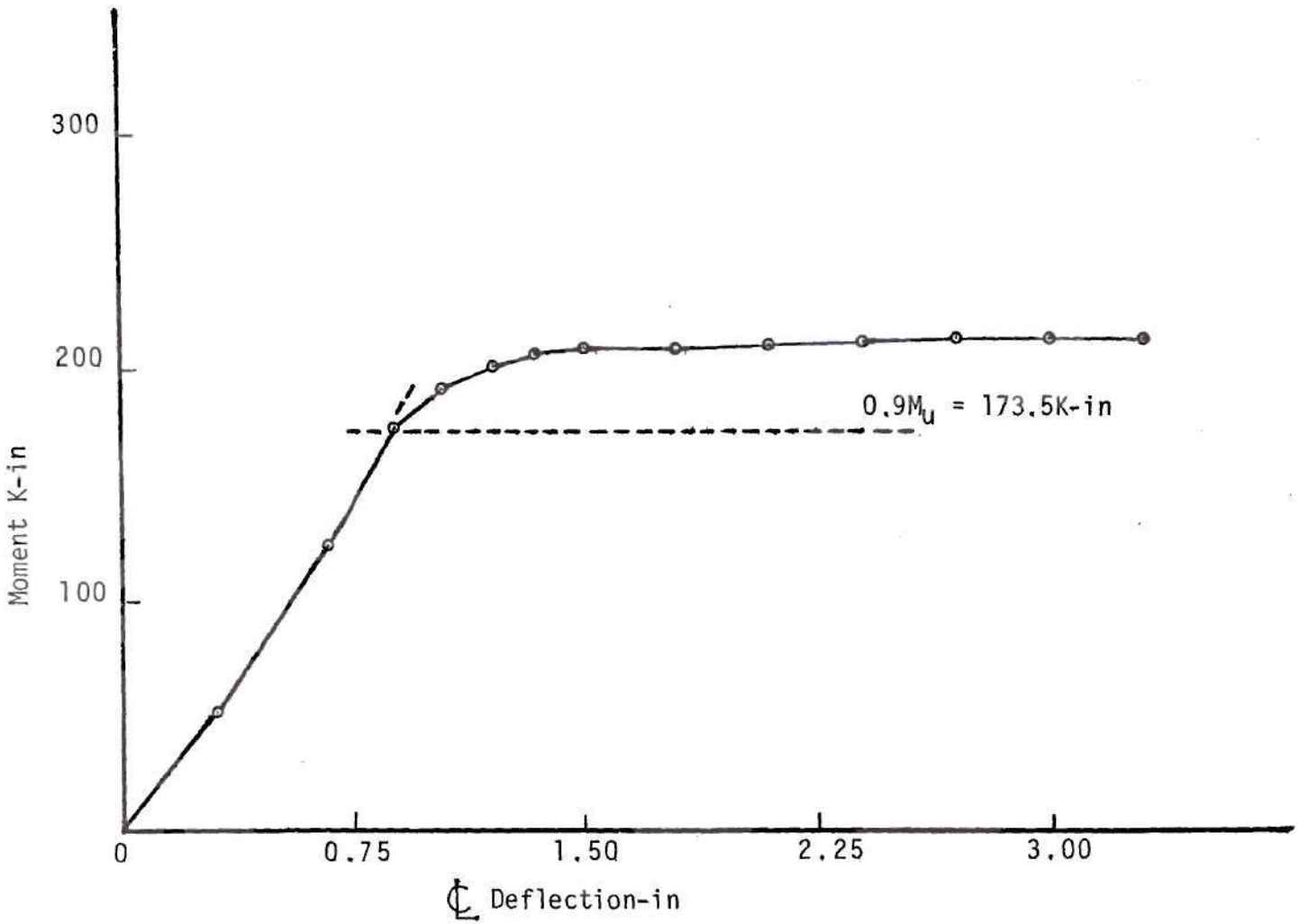

Figure 26. Moment-Deflection Relationship--0406F (11)

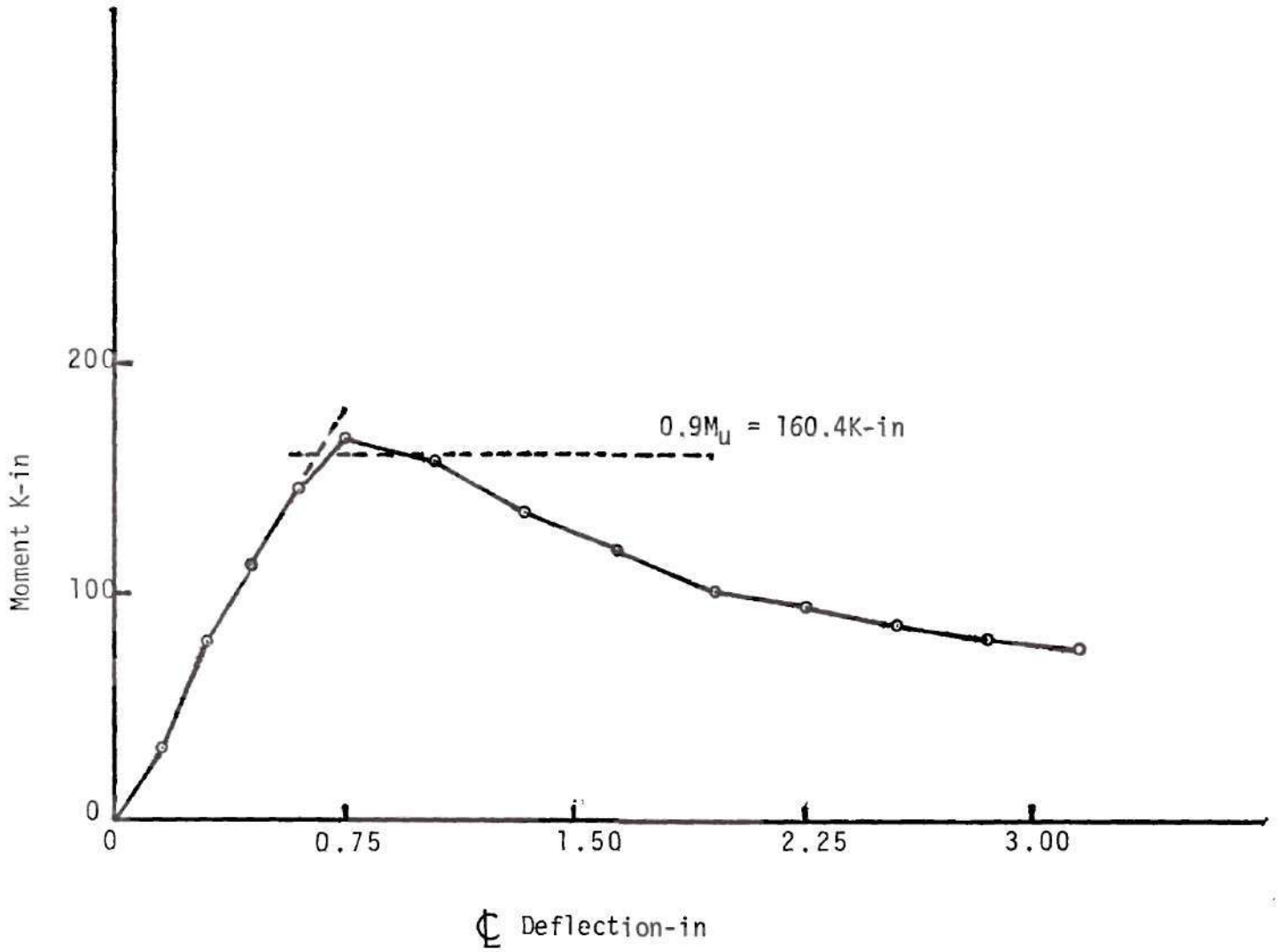

Figure 27. Moment-Deflection Relationship--0408F

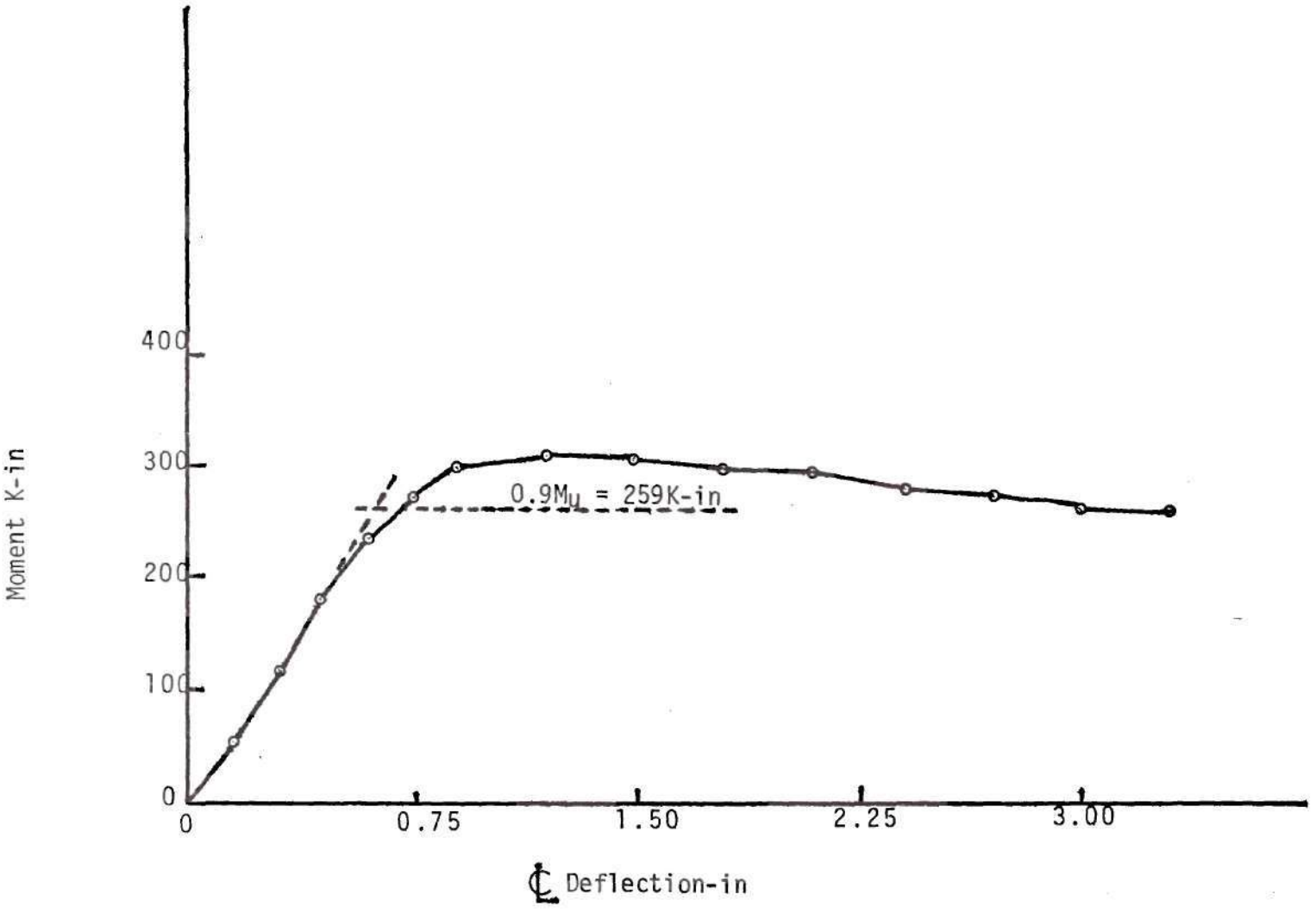

Figure 28. Moment Deflection Relationship--0408F (11)

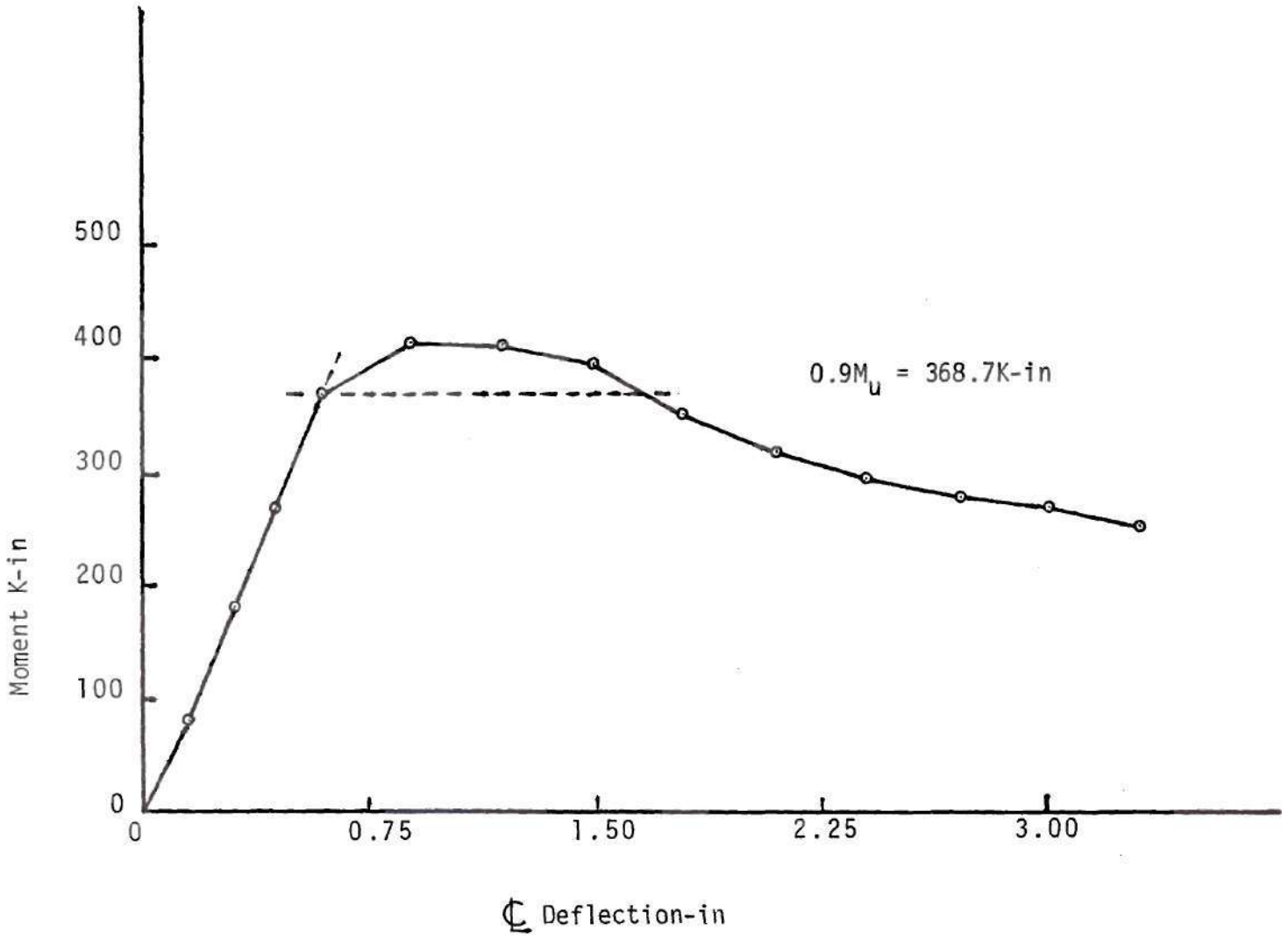

Figure 29. Moment-Deflection Relationship--0609F (11)

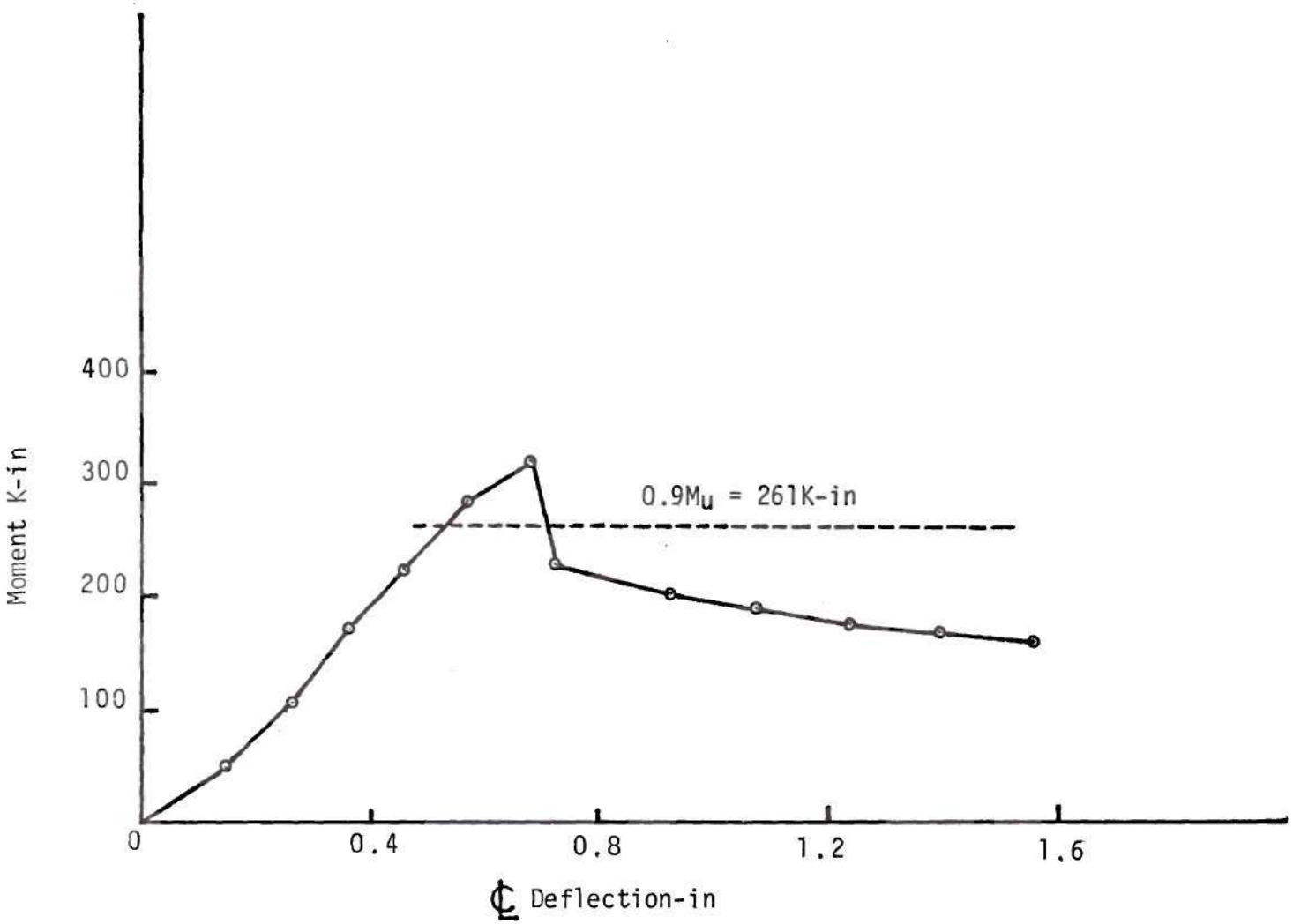

Figure 30. Moment-Deflection Relationship--0612F

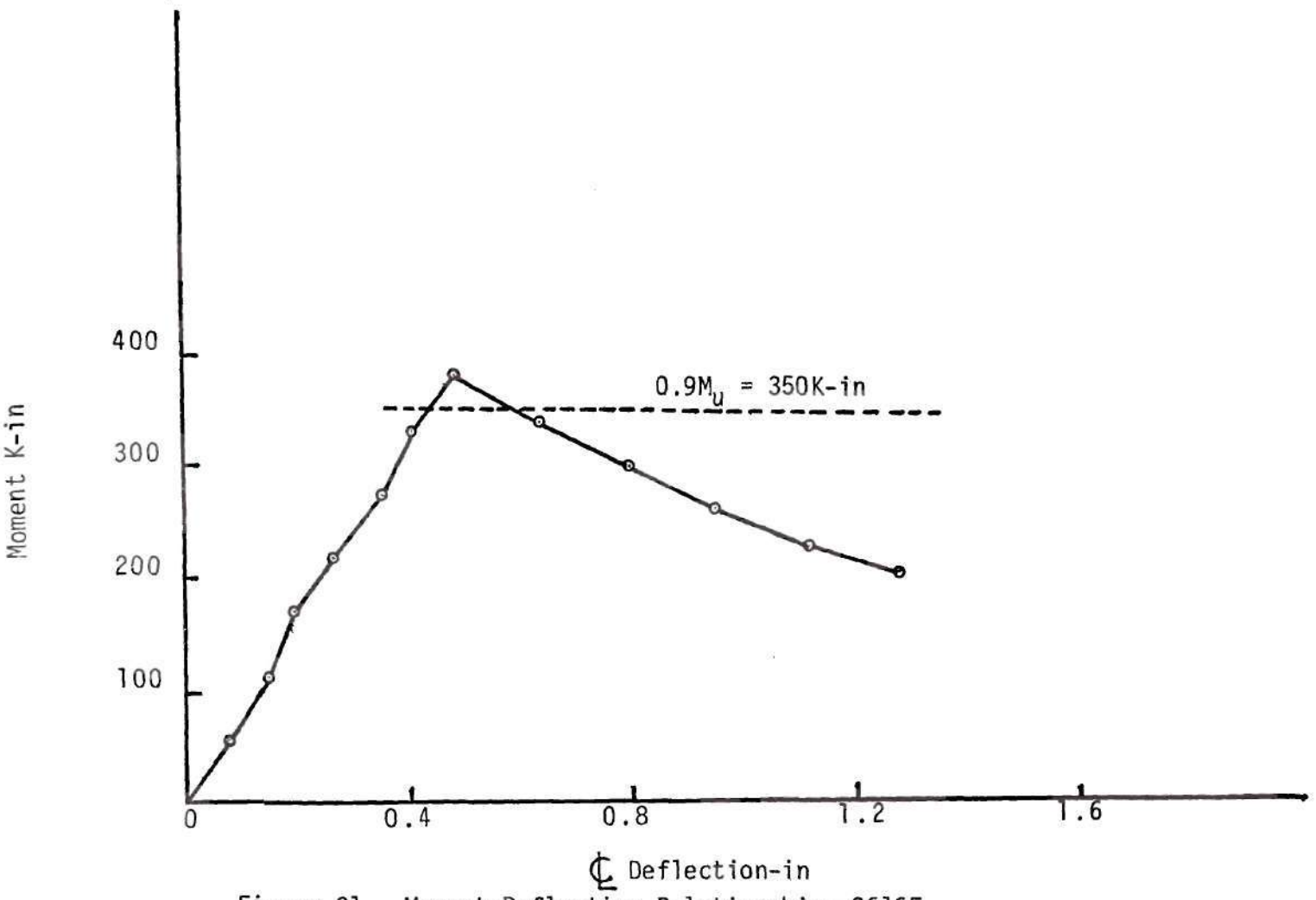

Figure 31. Moment-Deflection Relationship--0616F

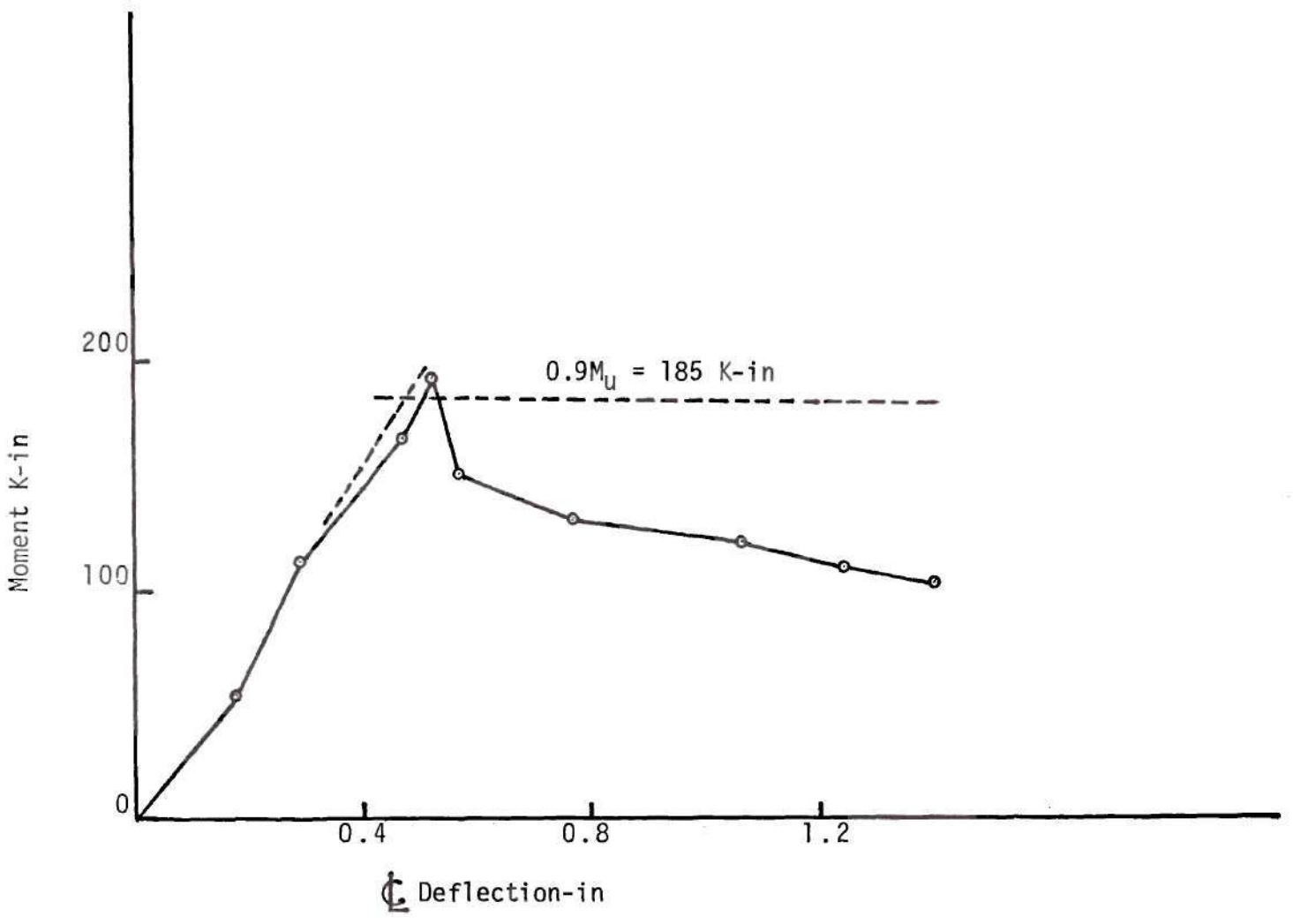

Figure 32. Moment Deflection Relationship--1008F

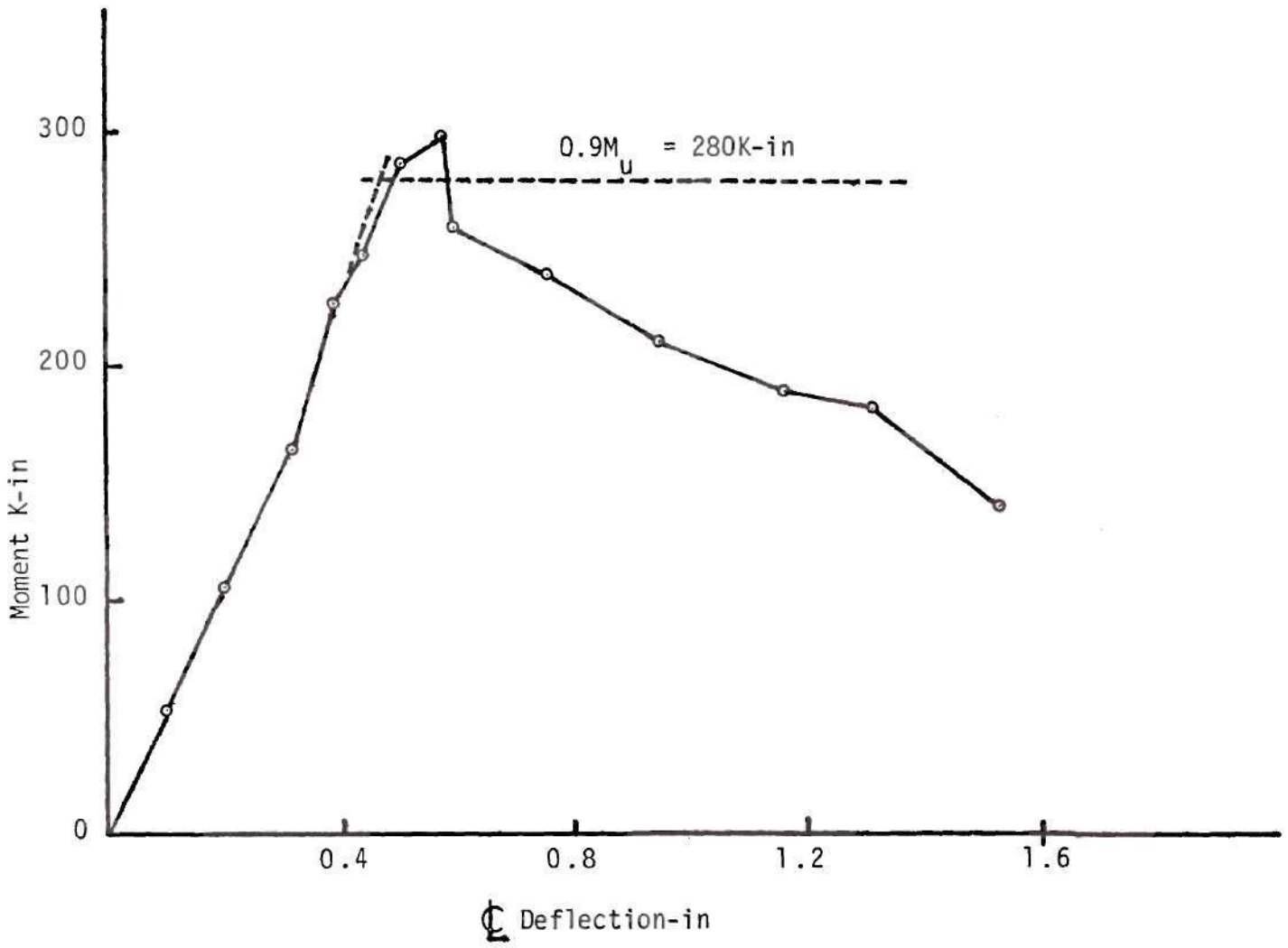

Figure 33. Moment Deflection Relationship 1012F

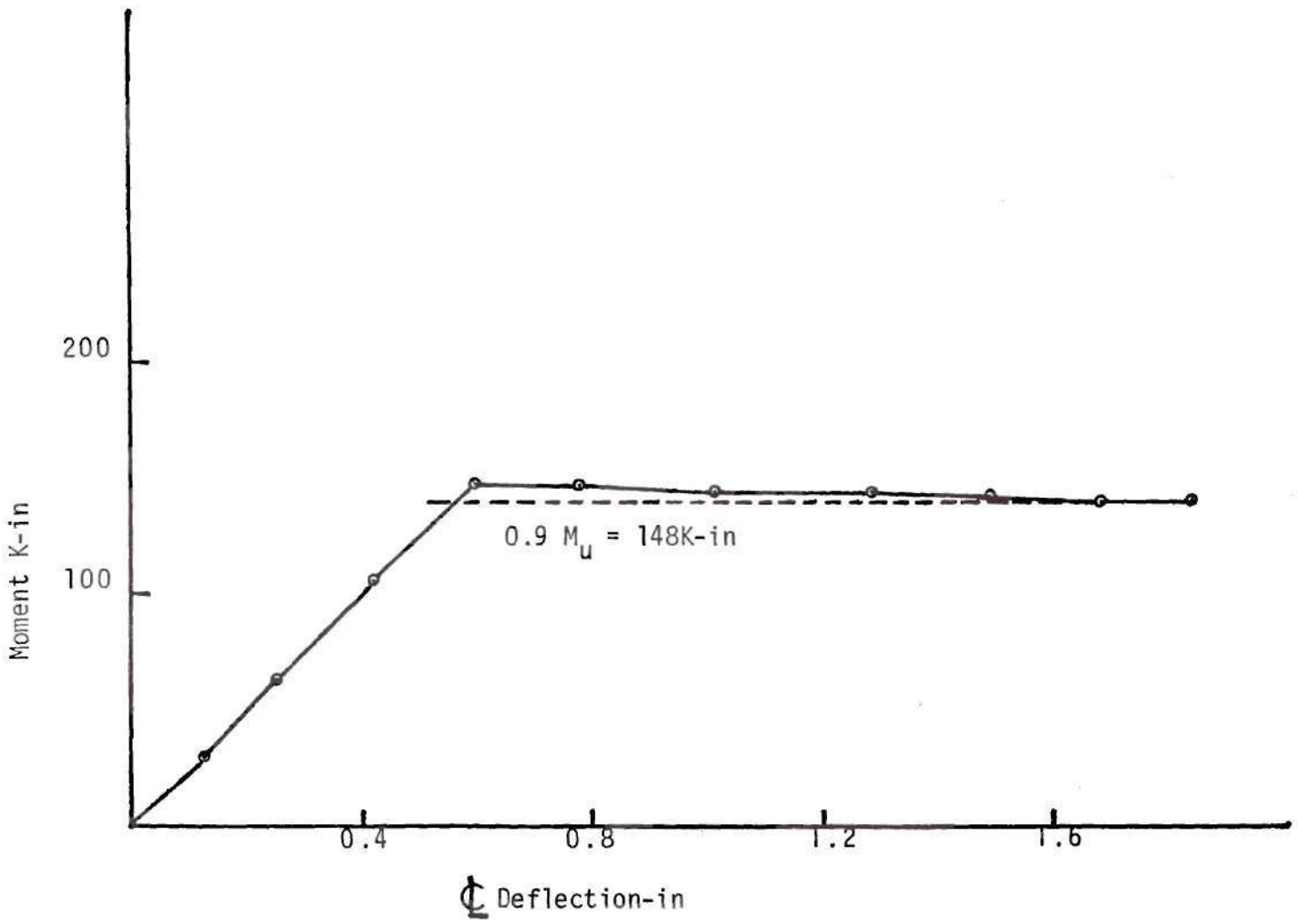

Figure 34. Moment--Deflection Relationship-0610W

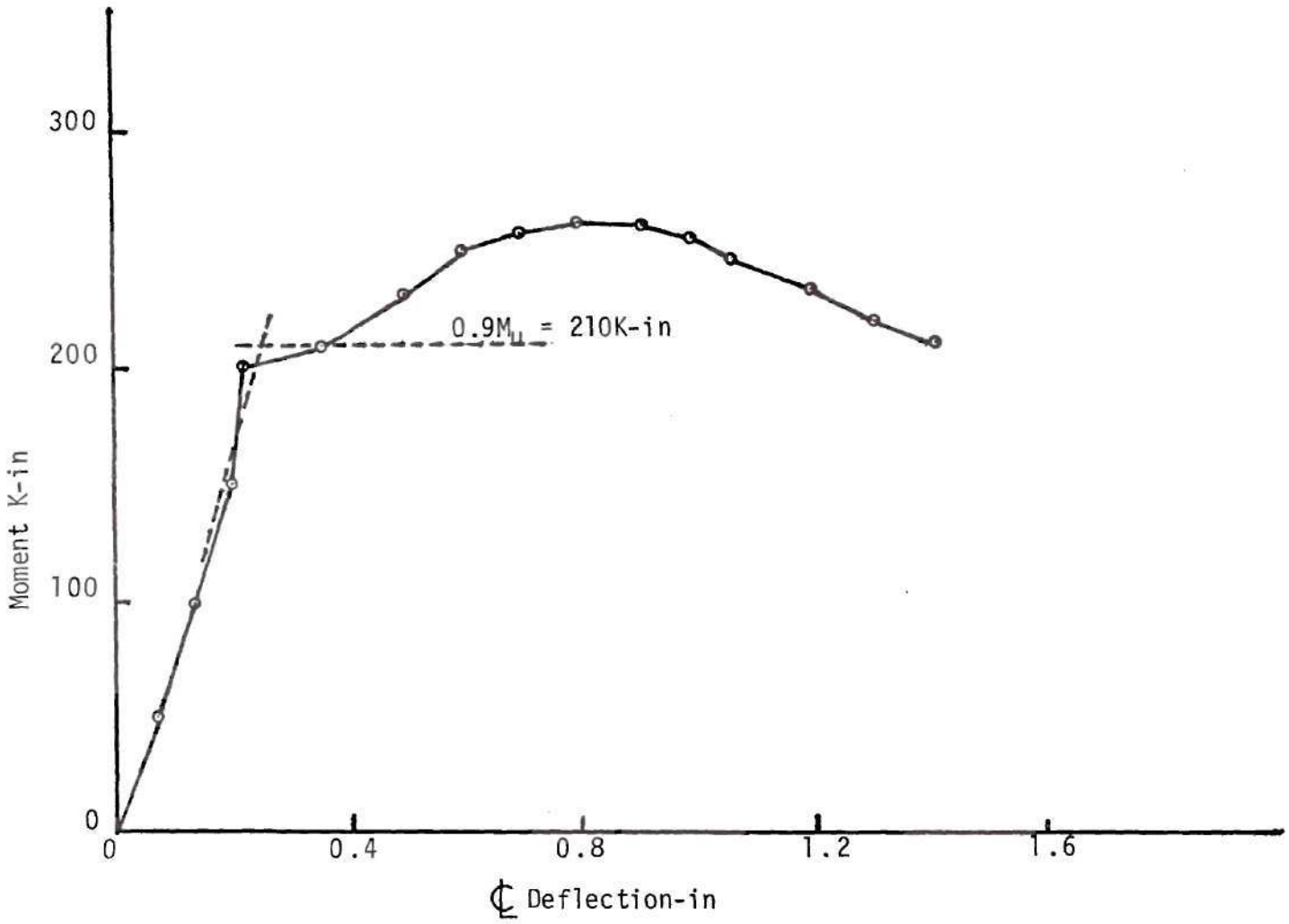

Figure 35. Moment Deflection Relationship-0815W

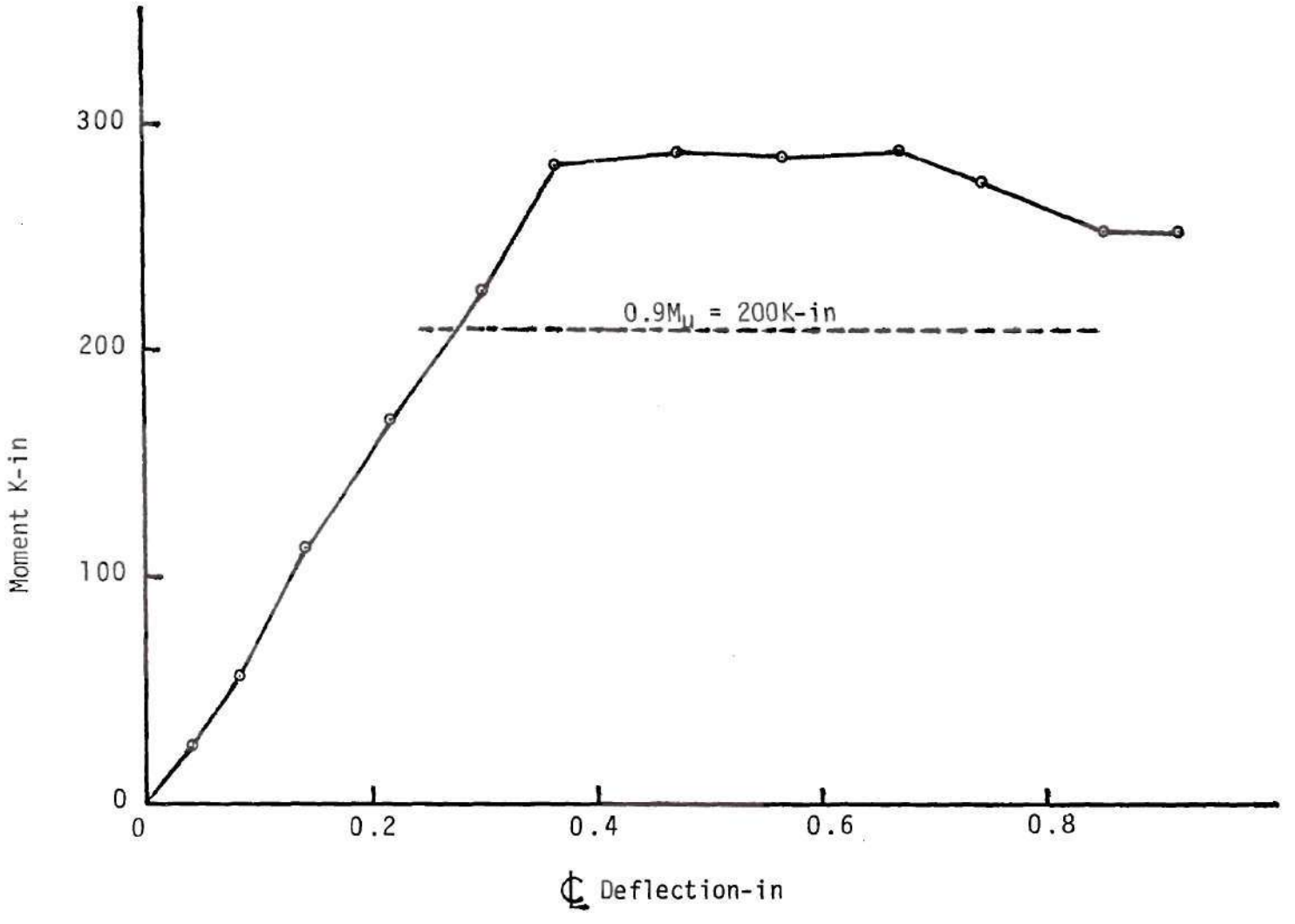

Figure 36. Moment-Deflection Relationship-1214W

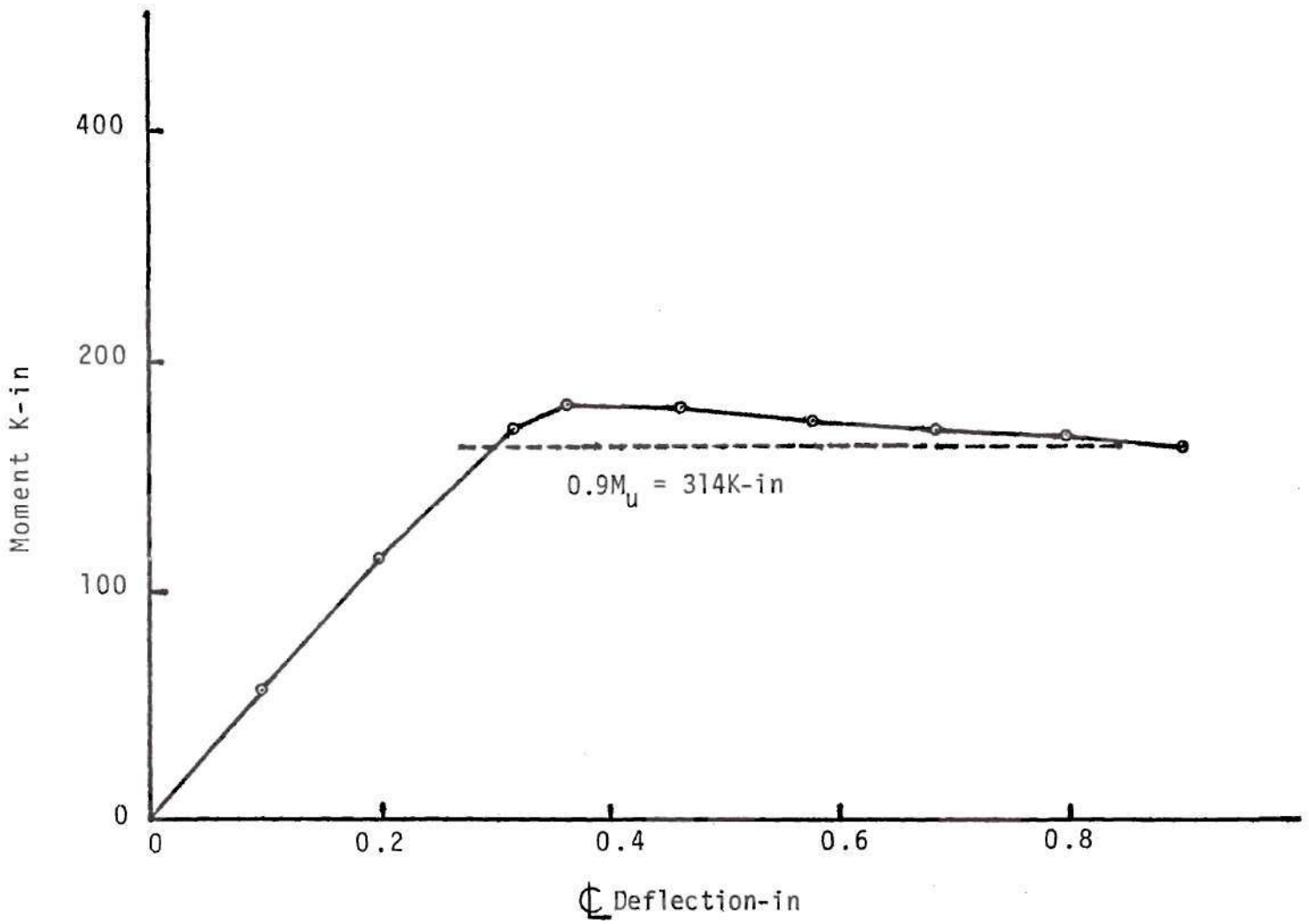

Figure 37. Moment Deflection Relationship-1218W

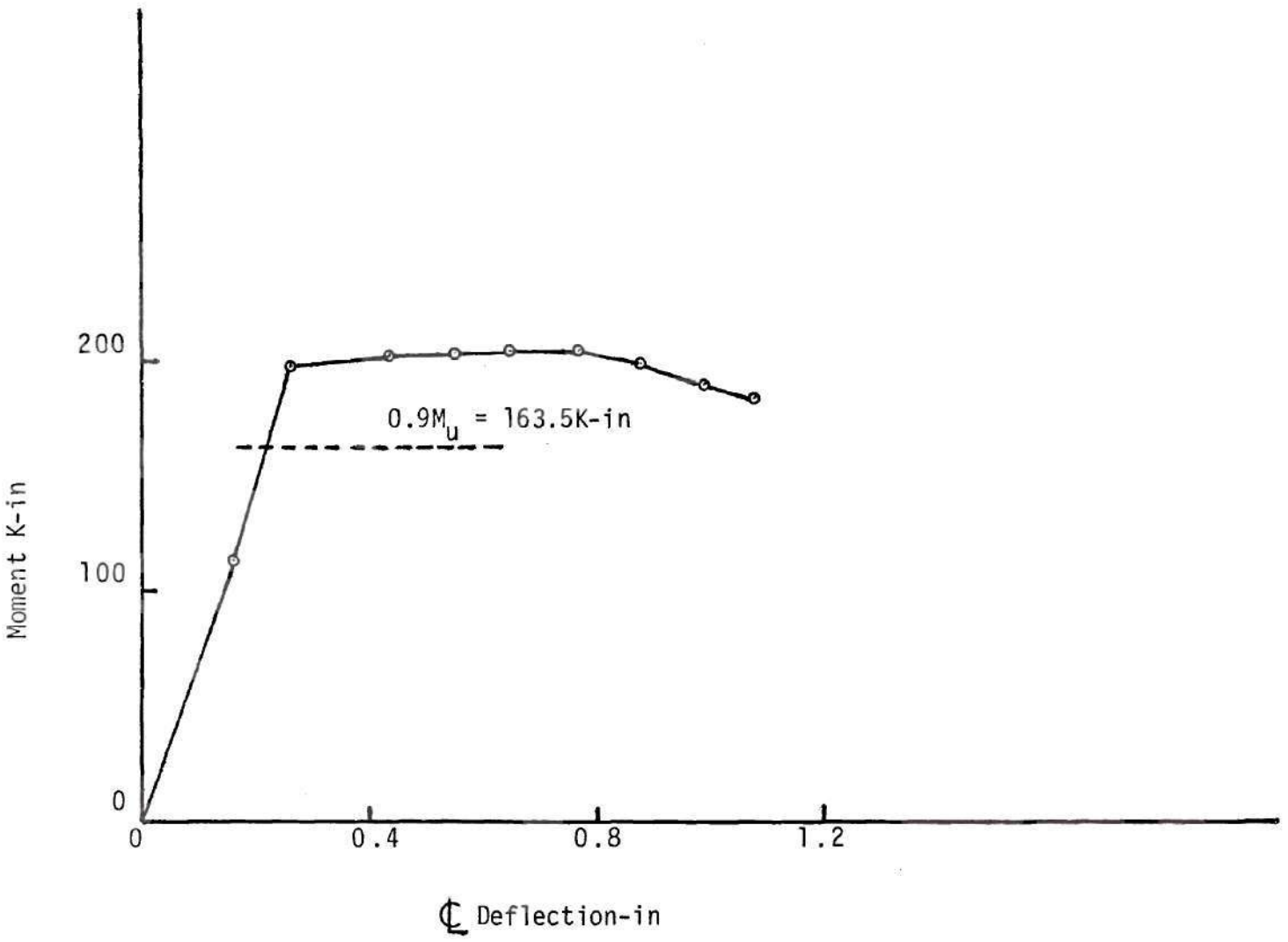

Figure 38. Moment Deflection Relationship-1610W

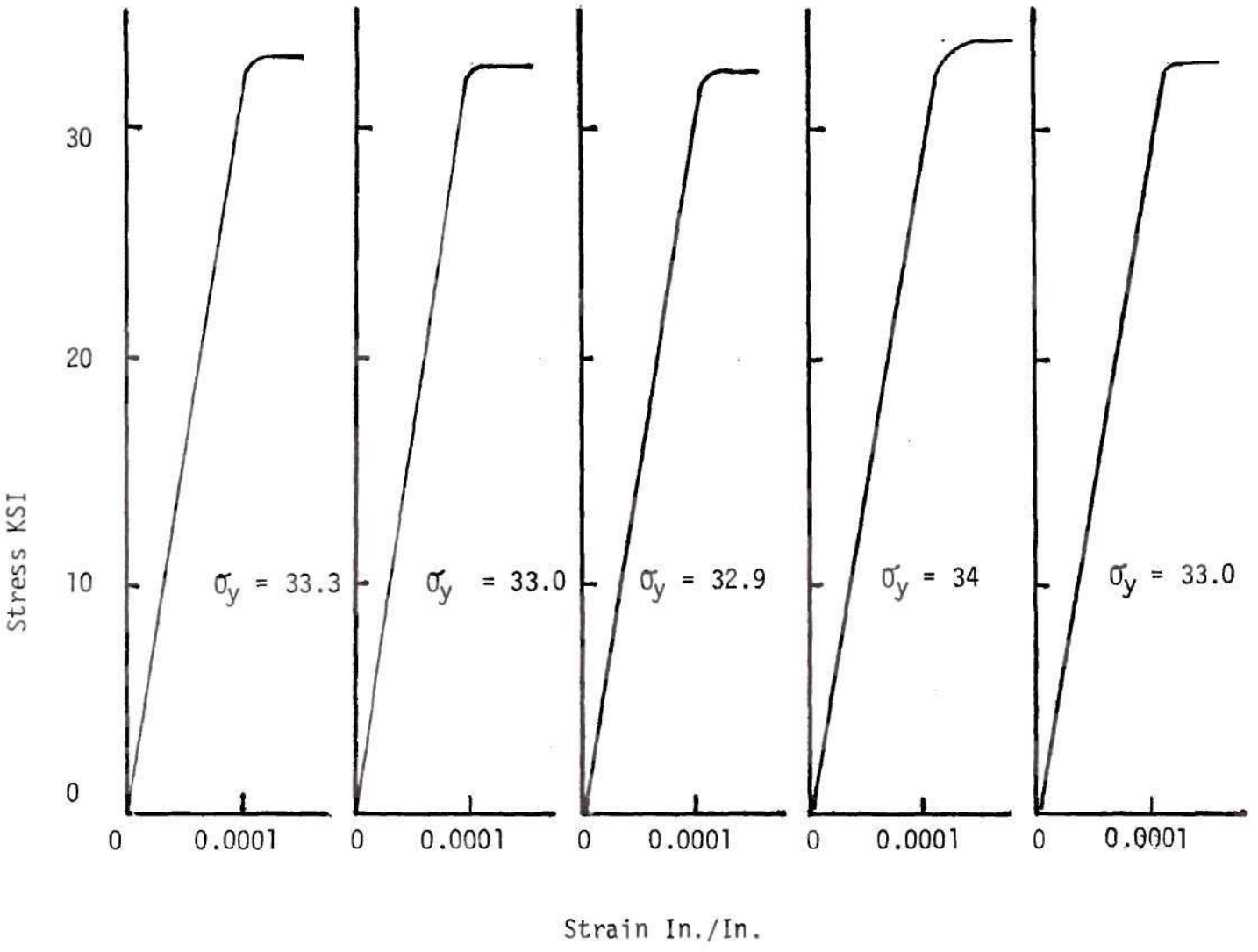

Figure 39. Results of Standard Coupon Tests

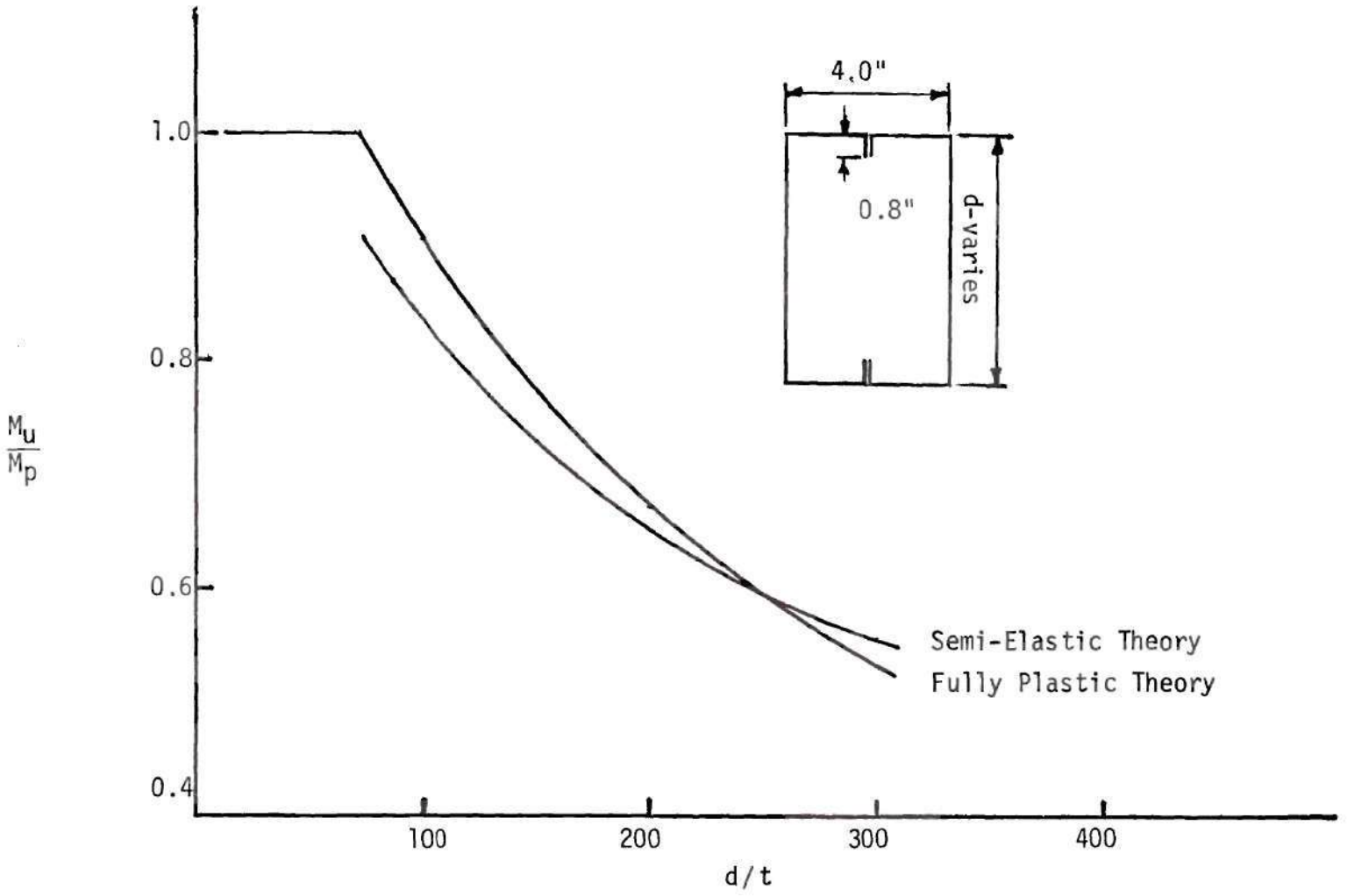

Figure 40. Reduction in Normalized Moment for Increasing Depth

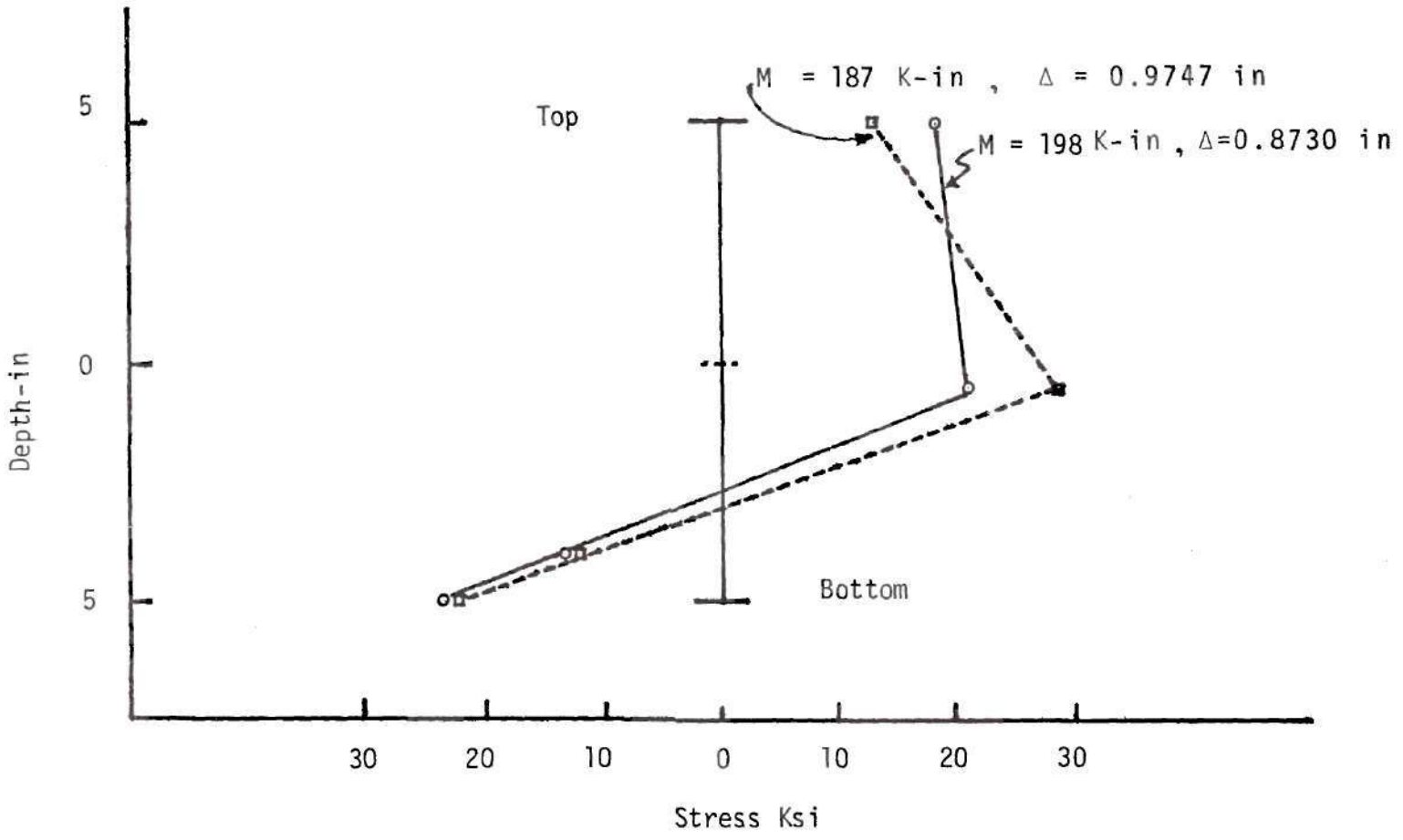

Figure 41. Stress Versus Depth-1610W

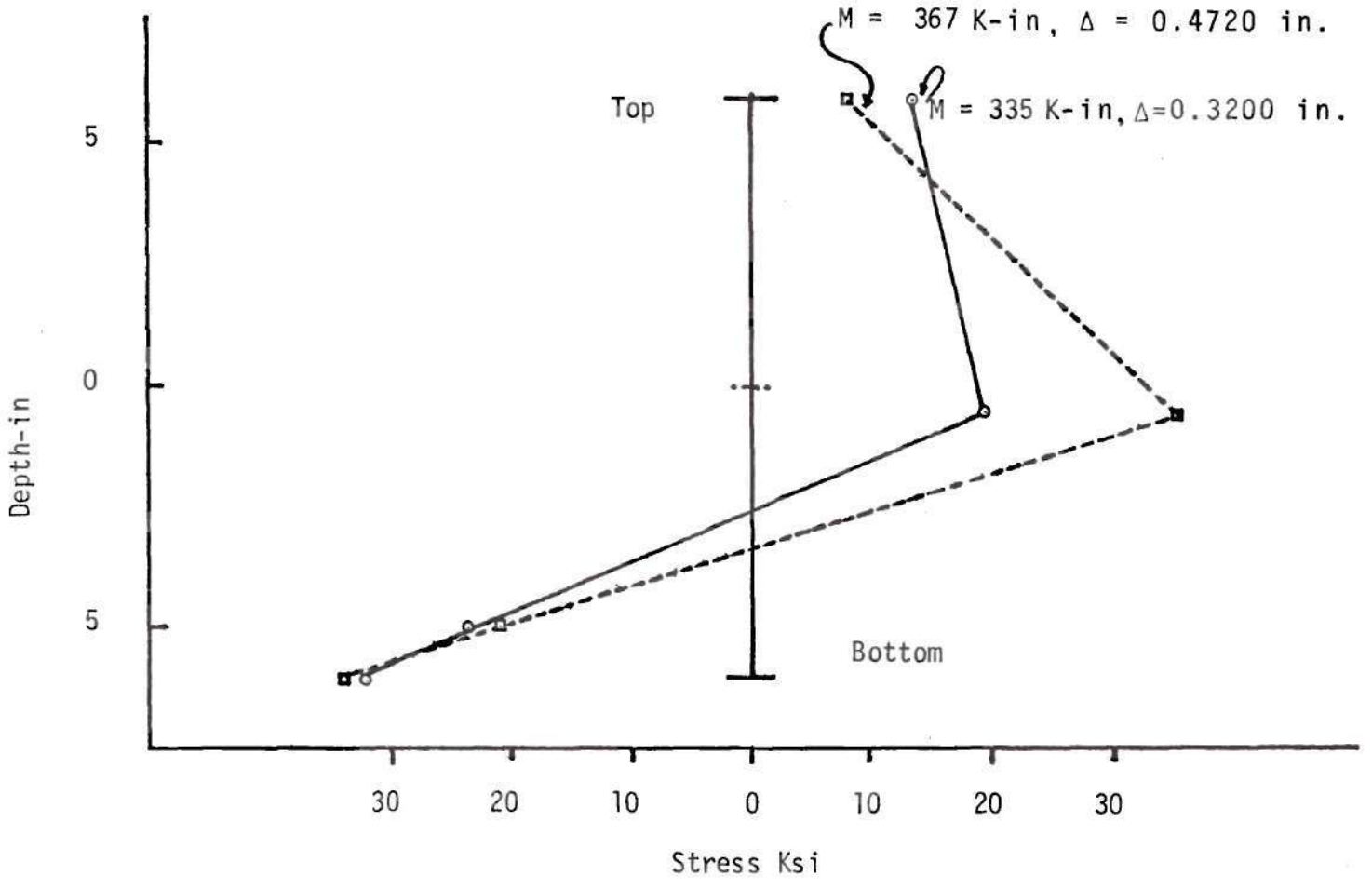

Figure 42. Stress Versus Depth-1218W

EXAMPLE NO. 1

Calculation of Ultimate Moment for Compact Section.

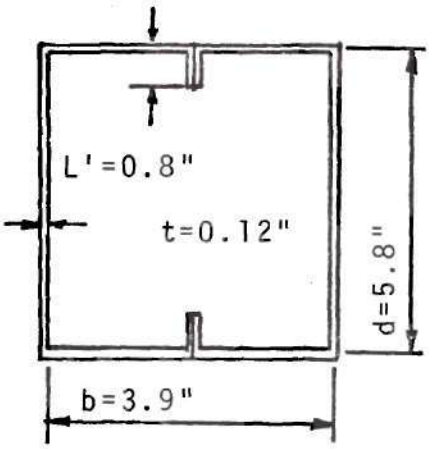

$$M_p = (bd + 2L\,(d-L) + \frac{d^2}{2})\,\sigma_y t$$

$$M_p = (3.9)(5.8) + 2\,(0.8)(5.8-0.8) + \frac{5.8^2}{2} \quad (33.4)\,(0.12)$$

$$M_p = 192.8 \text{ K-in}$$

EXAMPLE NO. 2

Calculation of Ultimate Moment for Non-Compact Beam Using the Fully Plastic Theory.

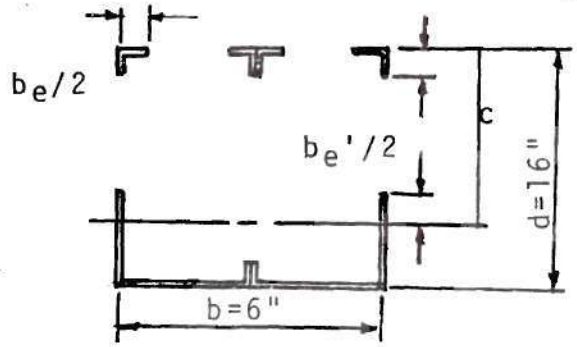

$$b_e = \frac{253}{\sqrt{\sigma_y}}\left[1 - \frac{50.3}{b/t\ \sqrt{\sigma_y}}\right] t$$

$$b_e = 3.27 - \frac{2.13}{3} = 2.56"$$

let $p = b + 2d - b_e - 6.54$

$$p = 6 + 32 - 5.12 - 6.54 = 26.35"$$

$$c = \frac{p + \sqrt{p^2+34}}{4}$$

$$c = 26.35 + \frac{\sqrt{26.35^2 + 34}}{4} = 13.33"$$

$$b_e' = 3.27 - \frac{2.13}{c} \qquad b_e' = 3.27 - \frac{2.13}{13.33} = 3.11"$$

$$M_u = \left[(b_e + b_e')c + (d-c)^2 + b(d-c) + 1.6(d-0.8)\right] t\sigma_y$$

$$M_u = \left[(2.56+3.11)13.33 + (16-13.33)^2 + 6(16-13.33) + 1.6(15.2)\right] 2.5$$

$$M_u = 389 \text{ K-in}$$

EXAMPLE NO. 3

Calculation of Ultimate Moment for Non-Compact Beam Using the Semi-Elastic Theory

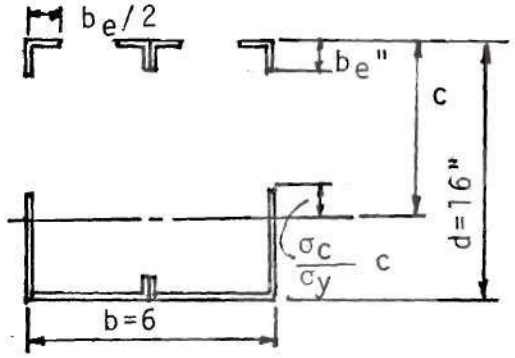

$$b_e = \frac{253}{\sigma_y}\left[1-\frac{50.3}{b/t\sqrt{\sigma_y}}\right] t$$

$$b_e = 3.27-\frac{2.13}{3} = 2.56"$$

$$c^2-2.34c^{4/3}-(b+2d+4L'+b_e)c+1.37c^{2/3}-2c^{-2}-356c^{-8/3}+23100c^{-6} = bd+d^2+2L'd$$

$$c = 9.074"$$

$$b_e" = 1.17c^{1/3}- 152c^{-3}$$

$$b_e" = 2.237"$$

$$\sigma_{cr}\ c/\sigma_y = 1.93"$$

$$I=2\left[\frac{\frac{\sigma_{cr}}{\sigma_y}c^3}{3} + \frac{(d-c)^3}{3}+b_e"\left(c-\frac{b_e"}{2}\right)^2+\frac{b_e c^2}{2}+0.8(c-0.4)+0.8(d-c-0.4)^2+\frac{b}{2}(d-c)^2\right] t$$

$$I = 104.5\ in^4$$

$$M_u = \frac{\sigma_y I}{c} = 384.7\ K\text{-}in$$

EXAMPLE NO. 4

Calculation of Ultimate Moment for Non-Compact Web Stiffened Beam.

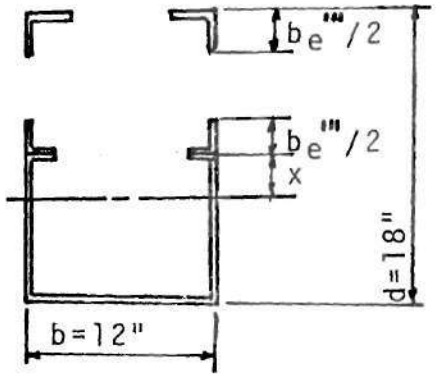

$b_e''' = 1.7$ in (from Figure 24)

$b_e''' = 1.7$ in (from Figure 24)

$$x = \frac{d(2b+d)}{4(b_e+2b_e'''+4L'+b+d)}$$

$$x = \frac{18(24+18)}{4(1.7+3.4+3.2+12+18)} = 4.93"$$

$$Mu = \left[b_e\left(\frac{d}{2}+x\right)+b_e'''\left(\frac{d}{2}+2x\right)+4L'x+\frac{2}{3}x^2+\frac{b}{x}\left(\frac{d}{2}-x\right)^2\ \frac{2}{3x}\left(\frac{d}{2}-x\right)^3\right] \sigma_y t$$

$$Mu = \left[1.7(9+4.93)+1.7(9+9.86)+3.2(4.93)+\frac{2}{3}(4.93)^2+\frac{12}{4.93}(9-4.93)^2+\right.$$

$$\left.\frac{2}{3}\ \frac{(9-4.93)^3}{4.93}\right] 25$$

$$Mu = 343 K\text{-in}$$

Required Rotation for Uniformly Distributed, Fixed-End Beam

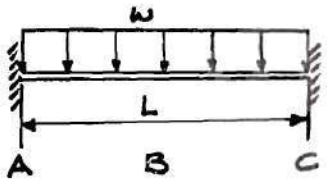

The Elastic Moment is greatest at the supports causing the first hinges to form there.

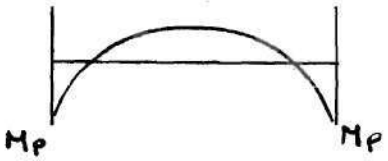

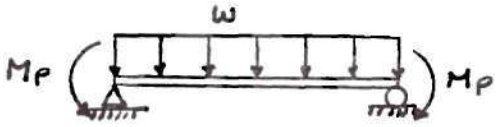

When a plastic hinge forms at the center, a mechanism will form. In the calculation of required rotation the hinge is considered to form at a point with the beam remaining fully elastic between hinges. The principles of slope-deflection will be used to determine the rotation at Point A when the moment at Point B reaches M_p.

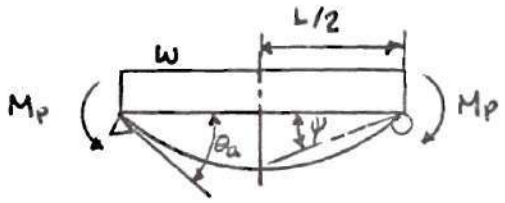

Writing the Slope-Deflection Equations for segment AB we have

$$M_{AB}=\frac{2EI}{L/2}\ (2\theta_A+\theta_B\ -\ 3\Psi)+W(L/2)^2/12. \tag{1}$$

and

$$M_{BA}=\frac{2EI}{L/2}\ (2\theta_B+\theta_A-3\Psi)+W(L/2)^2/12. \tag{2}$$

We are interested in the solution for the case when

$$M_{AB}\ =\ M_{BA}\ =\ M_P. \tag{3}$$

From symmetry we have

$$\theta_B\ =\ 0. \tag{4}$$

By summing moments about Point A on Segment AB we have

$$M_{AB}\ +\ M_{BA}\ =\ \frac{W\ (L/2)^2}{2} \tag{5}$$

Which when combined with Equation (3) yields

$$M_P\ =\ \frac{W(L/2)^2}{4}. \tag{6}$$

Combining Equations (2), (3), and (6) we have

$$\frac{W(L/2)^2}{4}=\frac{2EI}{L/2}\quad(\theta_A\ -\ 3\Psi\ )\ +\ \frac{W(L/2)^2}{12} \tag{7}$$

Which reduces to

$$-3\Psi\ =\ W(L/2)^3/12EI\ -\ \theta_A. \tag{8}$$

Substituting Equation (8) into Equation (1) we have

$$M_P = \frac{2EI}{L/2}\left(2\theta_A - \theta_A + \frac{W(L/2)^3}{12EI}\right) - \frac{W(L/2)^2}{12} \quad . \tag{9}$$

Solving for θ_A, we derive the required rotation capacity for the given beam:

$$\theta_A = \frac{M_p L}{6EI} \quad . \tag{10}$$

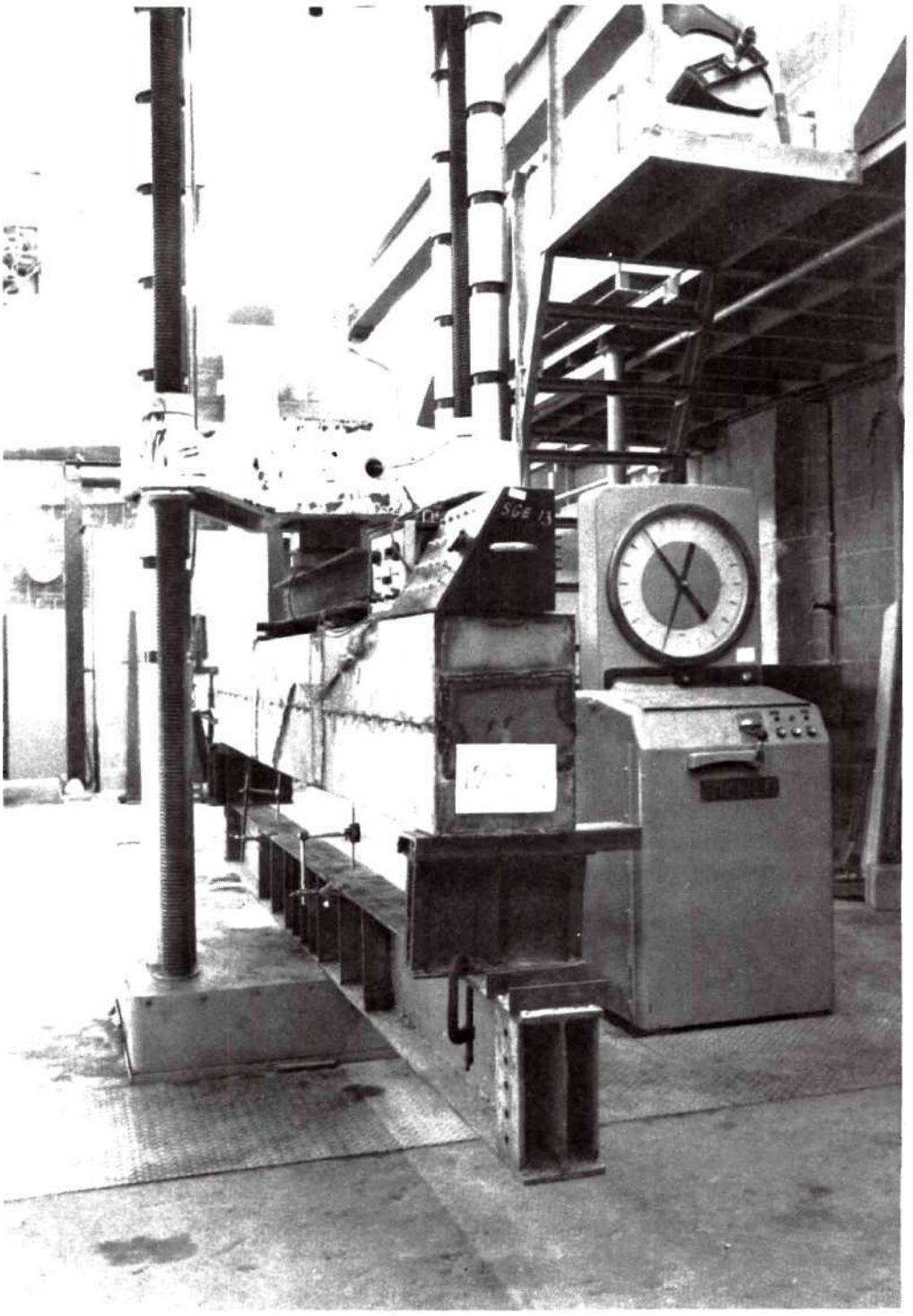

Figure 43. Actual Test Setup.

(a) Test Section 1816F (not used due to web crippling)

(b) Test Section 0616F

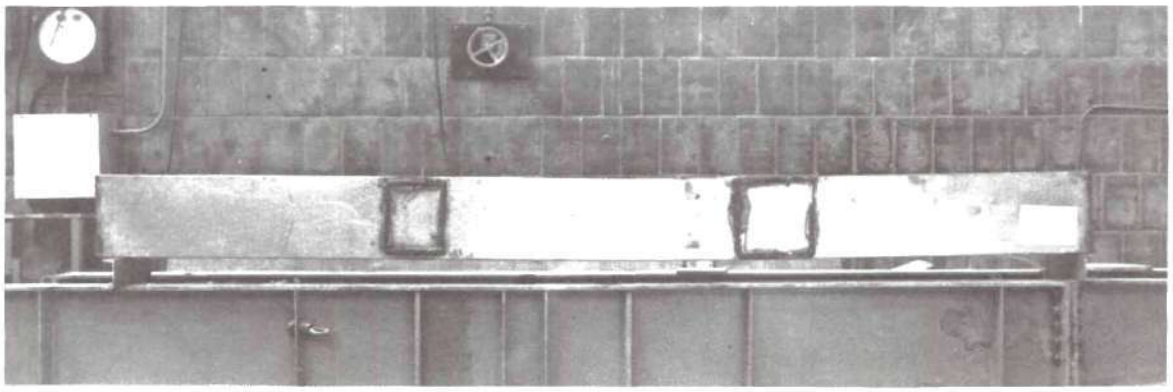

(c) Test Section 0612F

Figure 44. Test Sections

(a) Test Section 1008F

(b) Test Section 0609F(11)

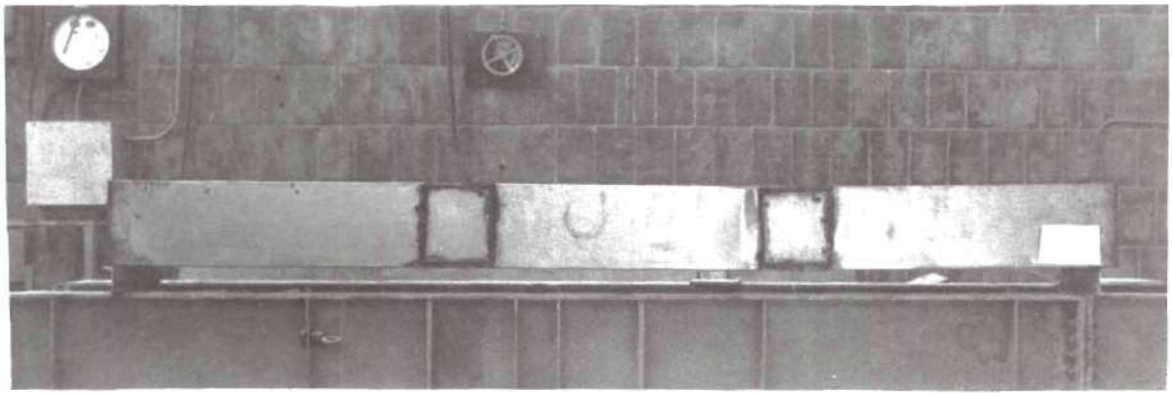

(c) Test Section 1012F

Figure 45. Test Sections

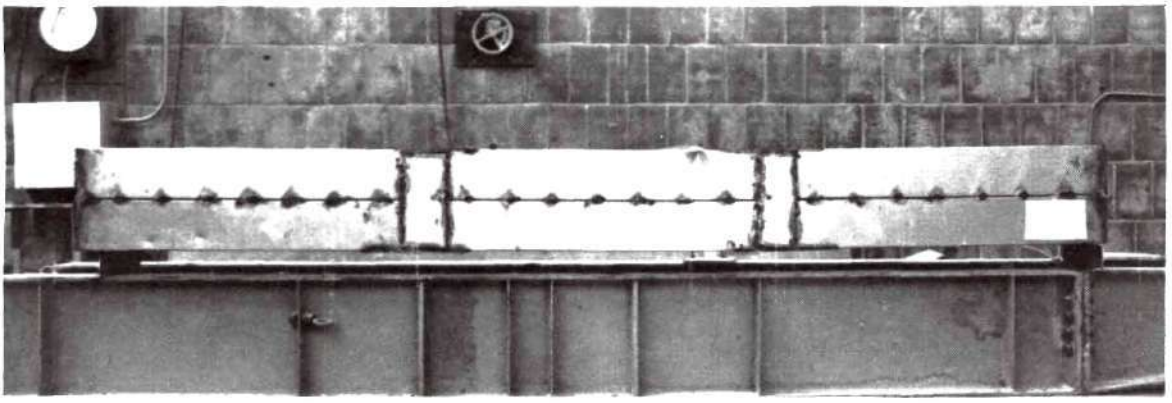

(a) Test Section 1214W

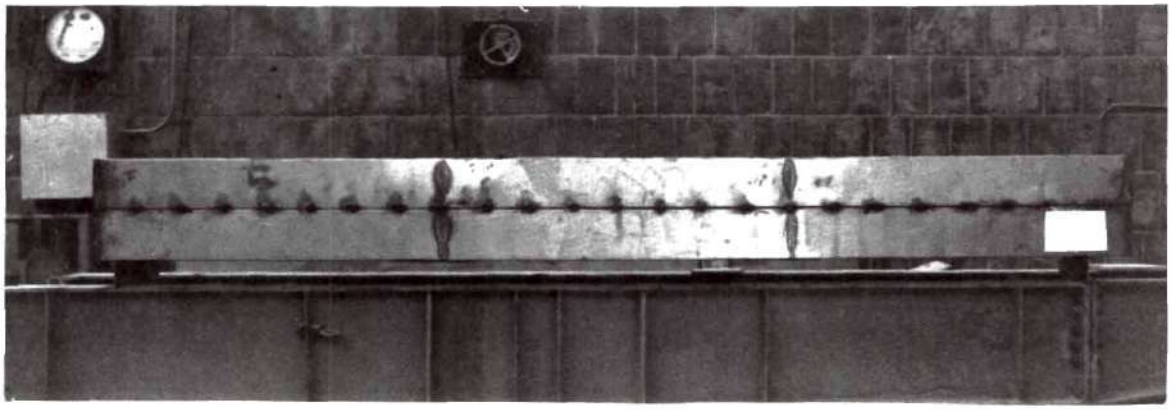

(b) Test Section 0815W

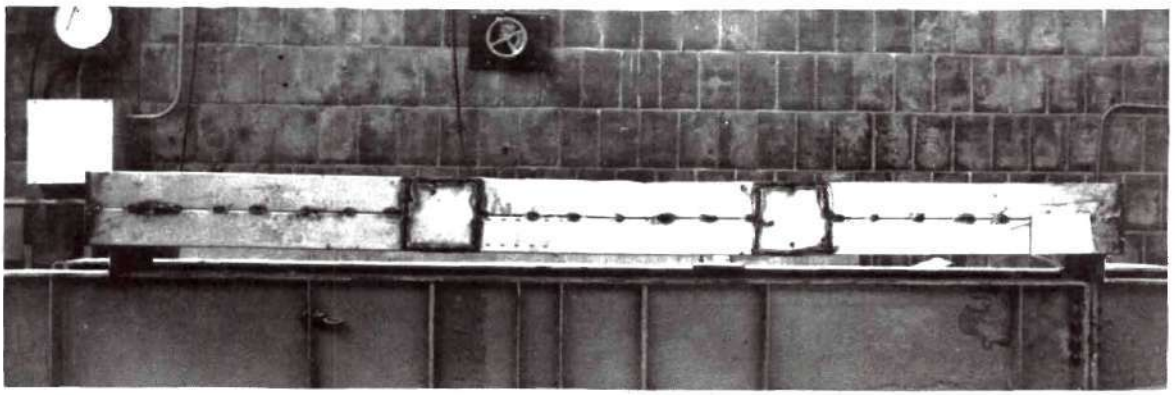

(c) Test Section 1610W

Figure 46. Test Sections

LITERATURE CITED

1. Adams, P.F., and Galambos, T.V., "Material Considerations in Plastic Design," Lehigh University, Fritz Labratory Report No. 297.23, November, 1966.

2. Basler, K., "Strength of Plate Girders in Bending." Trans. ASCE, Vol. 128, Part II (1963), pp 655-686.

3. Beedle, L.S., "Plastic Strength of Steel Frames," Lehigh University, Welded Continuous Frames and Their Components, Progress Report No. 14, February, 1955.

4. Beedle, L.S., Plastic Design of Steel Frames, Wiley, New York, 1958.

5. Bleich, F., Buckling Strength of Metal Structures, McGraw-Hill Book Co. Inc., New York, 1952.

6. Bulson, P.S., The Stability of Flat Plates, American Elsevier Publishing Co. Inc., New York, 1969.

7. Chajes, A., Britvec, S.J., Winter G., "Effects of Cold-Straining on Structural Sheet Steels," Journal of the Structural Divisions, ASCE, Vol. 89, No. ST2, April 1963, pp. 1-32.

8. Corrado, J.A. and Yen, B.T., "Failure Tests of Rectangular Model Steel Box Girders," Journal of the Structural Division, ASCE, Vol. 99, No. ST7, Proc. Paper 9854, July, 1973, pp. 1439-1955.

9. Croce, A.D., "The Strength of Continuous Welded Girders with Unstiffened Webs," The University of Texas at Austin, CESRL Thesis No. 70-2, January, 1970.

10. Driscoll, G.C., "Rotation Capacity Requirements for Beams and Portal Frames," thesis presented to Lehigh University, at Bethlehem, Pa., in 1958, in partial fulfillment of the requirements for the degree of Doctor of Philosophy.

11. Galambos, T.V., "Deformation and Energy Absorption Capacity of Steel Structures in the Inelastic Range," AISI, Bulletin No. 8, March, 1968.

12. Galambos, T.V., et. al. "Progress Report on Steel Box Girder Bridges," Journal of the Structural Division, ASCE, Vol. 97, No. ST4, Proc. Paper 8086, April , 1971, pp. 1175-1186.

13. Graves Smith, T.R., "The Ultimate Strength of Locally Buckled Columns of Arbitrary Length," Symposium on Thin-Walled Steel Structures, University College of Swansea, 1967.

14. Haaijer, G. and Thiirleman, B., "Local Buckling of Wide-Flange Shapes," Lehigh University, Fritz Laboratory, Progress Report X (not for publication) December, 1954.

15. Johnston, B.G., The Column Research Council Guide to Design Criteria for Metal Compression Members, 2nd Ed., John Wiley and Sons, Inc., New York, 1966.

16. Jairo, U. and Winter, G., "Cold Forming Effects in Thin-Walled Steel Members," Dept. of Structural Engineering, Cornell University, August, 1969.

17. Karren, K.W., "Corner Properties of Cold-Formed Steel Shapes," Journal of the Structural Division, ASCE, Vol. 93, No. ST1, February, 1967, pp. 401-432.

18. Karren, K.W. and Winter, G., "Effects of Cold-Forming on Light-Gage Steel Members," Journal of the Structural Division, ASCE, Vol. 93, No. ST1, February, 1967, pp. 433-469.

19. Ketter, R.L. and Beedle, L.S., "Moment-Rotation Chacteristics of Beam-Columns," Lehigh University, Fritz Laboratory Report No. 205A.11, November, 1952.

20. Kirkland, W.G., "Cold Roll Forming Practice in the United States," American Iron and Steel Institute, New York, 1966.

21. Korol, R.M. and Hudoba J., "Plastic Behavior of Hollow Plastic Sections," Journal of the Structural Division, ASCE, Vol. 98, No. ST5, Proc. Paper 8872, May 1972, pp. 1007-1023.

22. Lay, M.G., and Galambos, T.V., "Inelastic Steel Beams Under Uniform Moment," Journal of the Structural Division, ASCE, Vol. 91, No. ST6, Proc. Paper 4566, December, 1965, pp. 67-93.

23. Lay, M.G., "Yielding of Uniformly Loaded Steel Members," Journal of the Structural Division, ASCE, Vol. 91, No. ST6, Proc. Paper 4580, December, 1965, pp. 49-66.

24. Lay, M.G., "Some Studies of Flange Local Buckling in Wide-Flange Shapes," Lehigh University, Fritz Laboratory Report 297.10, July, 1964.

25. Lee, G.C., Ferrara, A.J., and Galambos, T.V., "Experiments on Braced Wide-Flanged Beams," Lehigh University, Fritz Laboratory Report No. 205H.6, March, 1963.

26. Reck, H.P., Pekoz, J., and Winter, G., "Inelastic Strength of Cold-Formed Steel Beams," Journal of the Structural Division, ASCE, Vol. 101, No. ST11, Proc. Paper 11713, November, 1975, pp. 2193-2703.

27. Shanley, F.R., "Inelastic Column Theory," Journal of the Aeronautical Sciences, Vol. 19, No. 5 (May, 1947) pp. 261-267.

28. Timoshenko, S.P. Strength of Materials, Vol. 2, Van Nostrand, 1st. ed., 1930, 2nd ed., 1941.

29. Timoshenko, S.P. Theory of Elastic Stability, McGraw-Hill Book Co., Inc., New York, 1936.

30. Tse, K.C., "Elastic and Inelastic Lateral-Torsional Buckling of Box Beams Subjected to Pure Bending," thesis presented to the Georgia Institute of Technology at Atlanta, Georgia, in 1971, in partial fulfillment of the requirements for the degree of Doctor of Philosophy.

31. Von Karman, T., Sechler, E.G., and Donnell, L.H., Trans. ASME, Vol. 54, 1932.

32. Walker, A.C. "Thin-Walled Structural Forms Under Eccentric Compressive Load Actions," thesis presented to the University of Glasgow at Glasgow, Scotland, in 1964, in partial fulfillment of the requirements for the degree of Doctor of Philosophy.

33. Yu, W.W., and Davis, C.S., "Cold-Formed Steel Members with Perforated Elements," Journal of the Structural Division, ASCE, Vol. 99, No. ST10, Proc. Paper 10059, October 1973, pp. 2061-2077.

34. "Specifications for the Design of Light Gage Steel Structural Members," Light Gage Cold-Formed Steel Design Manual, American Iron and Steel Inst., New York, 1968.

35. ASCE and WRC, Plastic Design in Steel--A Guide and Commentary, ASCE--Manuals and Reports in Engineering Practice-No. 41, 1971.

36. Specification for the Design, Fabrication and Erection of Structural Steel for Buildings, American Institute of Steel Construction, New York, 1969.

VITA

Jerry Lynn Householder was born April 5, 1943 in Seymour, Tennessee. He graduated from Young High School in 1961. He received a Bachelor of Science degree in Civil Engineering from the University of Tennessee in 1965. He received a Master of Science degree in Civil Engineering from the Georgia Institute of Technology in 1967. He has served on the faculty of Auburn University and as chief engineer for the Christian Testing Laboratories. He is currently engaged in private business; he is married and has two children.